

# **EVALUATION OF STAINLESS STEEL CLAD REINFORCING BARS**

**By  
David Darwin  
Carl E. Locke, Jr.  
Javier Balma  
Jason T. Kahrs**

**A Report on Research Sponsored by  
STRUCTURAL METALS, INC.**

**Structural Engineering and Engineering Materials  
SL Report 99-3**

**UNIVERSITY OF KANSAS CENTER FOR RESEARCH, INC.  
LAWRENCE, KANSAS  
July 1999**

# EVALUATION OF STAINLESS STEEL CLAD REINFORCING BARS

## ABSTRACT

The corrosion performance of stainless steel clad reinforcing bars provided by Structural Metals, Inc. is compared with that of conventional (black) reinforcement. 304 stainless steel is used as the cladding material. The No. 19 [No. 6] bars are compared using rapid corrosion potential and macrocell tests. The tests are carried out in two stages, first with bare reinforcement and then with reinforcement encased in mortar. Test specimens are placed in simulated concrete pore solution with a 1.6 molal ion concentration of sodium chloride. The continuity and uniformity of the cladding is measured using a scanning electron microscope.

The study indicates that the cladding provides a significant improvement in corrosion performance, if the mild steel core of the clad bars is adequately isolated from chlorides. For bars not encased in mortar, the corrosion rate of the clad bars ranges between 0 and 0.3  $\mu\text{m}/\text{yr}$ , about  $1/_{100}$  of the value observed for the black bars. For bars encased in mortar, the corrosion rate averages 0.1  $\mu\text{m}/\text{yr}$ ,  $1/_{20}$  to  $1/_{50}$  of the value exhibited by the black steel. Cladding thickness varies between 0.196 and 0.894 mm (7.7 and 35 mils), averaging 0.467 mm (18 mils). Based on an average corrosion rate of about 0.2  $\mu\text{m}/\text{yr}$  for stainless steel bars not embedded in mortar (representing the corrosion rate that would be expected at a void adjacent to a bar in concrete), the cladding appears to be satisfactory if the current minimum thickness is maintained. Tests of bars clad with 316 stainless steel and longer-term tests are recommended.

## **INTRODUCTION**

The corrosion performance of stainless steel clad and uncoated (black) No. 19 [No. 6] reinforcing bars is compared using rapid corrosion potential and macrocell tests. The purpose of the tests is to obtain an initial evaluation of the clad reinforcement for application in severe corrosion environments, such as reinforced concrete subjected to deicing chemicals or saltwater. Results include 19 stainless steel clad and 17 black bar tests for bare bars and 13 each stainless steel and black bar tests for bars cast in mortar.

In addition to evaluating the corrosion performance of the clad reinforcing steel, the uniformity of the cladding thickness is evaluated using a scanning electron microscope.

The study indicates that the cladding provides significant corrosion protection if it is fully intact. Details of the study follow.

## **EXPERIMENTAL WORK**

### **Materials**

The reinforcing steel consisted of hot-rolled, stainless steel clad and uncoated No. 19 [No. 6] bars. A total of 80 lineal feet of black steel and 85 lineal feet of clad reinforcement were provided. The cladding consisted of 304 stainless steel that had been sprayed on the surface of a portion of a billet. The partial billet was welded to a full mild steel billet, which was then rolled in the normal fashion. The region of the billet that was sprayed with the stainless steel produced the clad reinforcement.

The thickness and continuity of the cladding was evaluated using a scanning electron microscope. The corrosion-resistant properties of the reinforcement were evaluated by comparing the corrosion potential and rate of corrosion in a macrocell of the clad reinforcement with that of the conventional reinforcement. Details of the procedures are described next.

## Scanning Electron Microscope Study

Sections of the reinforcement were removed and polished to obtain scanning electron microscope specimens to determine the continuity of the cladding. Polishing was carried out using (progressively) 150, 300, 600, 1000, and 2000 grit carborundum paper. The specimens were mounted on an aluminum stub and imaged using a backscattered electron detector on a Philips SEM 515 scanning electron microscope. Images were obtained using an ELMDAS digital image acquisition system with a pixel density of 512 x 512 and a pixel dwell time of 131 to 915 microseconds at an accelerating voltage of 20 kV and probe diameter of 200 nm.

Cladding was measured at 60 points around the periphery of the bar on six specimens. Magnifications between 11.6x and 186x were used.

## Rapid Corrosion Potential and Time-to-Corrosion Tests

These tests are run with both plain reinforcing bars (Stage 1) and bars embedded in a cylinder of mortar (Stage 2). In the latter case, the contact surface between the mortar and the bar simulates the contact obtained between concrete and reinforcing bars in actual structures. A test specimen consists of a 127 mm (5 in.) long No. 19 [No. 6] reinforcing bar. The bars used in Stage 2 (Fig. 1) are symmetrically embedded 76 mm (3 in.) in a 38 mm (1.5 in.) diameter mortar cylinder. In one case for each type of bar, the mortar cylinder is 30 mm (1.18 in.) in diameter. To guard against crevice corrosion, a 15 mm (0.6 in.) wide ring of epoxy is painted around the region of the bar where it exits from the mortar. The cylinder is 102 mm (4 in.) long. The overall length of the specimen is 153 mm (6 in.). The mortar has a water-cement ratio of 0.50 and a sand-cement ratio of 2. It is manufactured with Type I portland cement, graded sand meeting the requirements of ASTM C 778, and deionized water.

*Corrosion potential test* – The corrosion potential test requires two plastic containers (Fig. 2). The test specimen is placed in a 3.8-liter (4 qt) container filled to a depth that exposes 63 mm (2.5 in.) of the steel to a simulated pore solution with a 1.6 molal (m) ion concentration of sodium chloride. A standard Calomel reference electrode is placed in a separate container, along with a



saturated potassium chloride solution. The two containers are connected by a salt bridge and the potential (voltage) of the steel with the respect to the Calomel electrode is measured daily using a voltmeter. The voltage is called the corrosion potential of the steel.

The simulated pore solution (17.84 g of sodium hydroxide and 18.81 g of potassium hydroxide per liter of solution) represents the liquid in the saturated pores and capillaries of concrete (Farzammehr 1985). The salt bridge allows for the completion of the corrosion cell when the corrosion potential is measured.

*Macrocell test* – To obtain a rapid measure of the degree of corrosion that occurs through the formation of a macrocell, the corrosion potential test is modified (Fig. 3) so that the container with the Calomel electrode is replaced by another container with two specimens immersed in simulated pore solution (with no chlorides added). The test specimen in the pore solution with sodium chloride (anode) is electrically connected through a 10-ohm resistor to the two specimens in the simulated pore solution (cathode). The macrocell test specimen is completed by a salt bridge that connects the liquid in the two containers. Air (scrubbed to remove  $\text{CO}_2$ ) is bubbled into the liquid surrounding the cathode to ensure an adequate supply of oxygen.

A minimum of six replications were used for each combination of test variables.

The ends of the steel in the specimens used in both Stages 1 and 2 were either covered with a two-component epoxy of the type used to patch epoxy-coated reinforcement (Herberts O'Brien Nap-Guard Rebar Patch Kit) or with a plastic cap, closely matching the diameter of the specimen, that was filled with the epoxy prior to placement on the end of the bar. The purpose in both cases was to limit corrosion to the deformed surface of the reinforcement. In the case of black steel, it is generally understood that the presence of mill scale gives some improvement to the corrosion performance of the steel. Thus, exposing a cut end alters the test results. In the case of the clad reinforcement, exposure of the mild steel core significantly decreases the corrosion performance of the bar. This point is addressed at greater length in the Results section of the report.

Specimens were held upright with a styrofoam support. A mortar fill, matching that used in the specimens, was placed in the containers for tests involving bars embedded in mortar.

Corrosion potential tests lasted for 40 days, while macrocell tests lasted for 100 days.

## RESULTS AND EVALUATION

### Cladding Thickness

The images obtained with the scanning electron microscope are shown in Figs. 4-14. Figs. 4-7 show the variation in cladding thickness on longitudinal sections that cut through transverse ribs. Figs. 8-10 show the variation in cladding thickness for transverse sections cut through the barrel of the bar. The measurements summarized in Table 1 indicate that the cladding thickness varied between 0.196 and 0.894 mm (7.7 and 35 mils), with an average of 0.467 mm (18 mils). As shown in Figs. 11-13, the cladding tends to form an indent in the vicinity of the longitudinal rib with a depth of about 1.8 to 2 mm (71 to 79 mils). The indent exhibits a longitudinal crack that penetrates 1 to 1.4 mm (39 to 55 mils), less than the total depth of the indent and, thus, not penetrating to the mild steel core. In most cases, the cladding and the mild steel appear to be closely bonded. However, at one location, shown in Figs. 13 and 14, a 1.5  $\mu\text{m}$  wide crack was observed between the two metals near the indentation.

### Corrosion Tests

*Stage 1* – The results for Stage 1 are shown in Figs. 15-29. The figures demonstrate that the stainless steel clad bars exhibit significantly less corrosion than the black steel bars, as long as the cut ends of the bars are properly protected. Figures 15-18 show the results of the **corrosion potential tests** for the black steel bars. The ends of specimens PB-1 through PB-6 (Figs. 15-17) were coated with epoxy. The ends of specimens PBC-1 and PBC-2 (Fig. 18) were protected with a plastic cap filled with epoxy. In all cases, the corrosion potential rapidly changes to  $-0.5$  V, indicating a potential for rapid corrosion.

The corrosion potential test results for the stainless steel clad bars are shown in Figs. 19-22. Like the PB specimens, the ends of the PS specimens were coated with epoxy, and like the PBC

PBC specimens, the ends of the PSC specimens were protected with a plastic cap filled with epoxy. A corrosion potential of  $-0.2$  V indicates passivation of the steel surface and a low likelihood of corrosion. More negative potentials indicate a greater tendency toward corrosion. As shown in Figs. 19-21, only one specimen, PS-2, became fully passive. The other specimens indicate a potential to corrode. However, without exception, the nonpassivated specimens exhibited corrosion products at the edge of the epoxy coating at the end of the bar. The passive specimen did not. As shown in Fig. 22 for specimens PSC-1 and PSC-2 (ends protected with plastic caps filled with epoxy), a passive condition was rapidly attained and maintained for the full 40 days of the corrosion potential test.

The results for the **macrocell tests**, shown in Figs. 23-29, provide results that match those in the corrosion potential tests. The corrosion rate in the macrocell tests for the black steel reinforcement initially attains a value as high as  $40 \mu\text{m/yr}$ , fluctuating between 10 and  $40 \mu\text{m/yr}$  over the 100 day period of the test.

The corrosion rates for the stainless steel bars, however, are highly variable. The results, shown in Figs. 25-27 for specimens MS-1 through MS-8, indicate that three specimens, MS-3, MS-6, and MS-7, exhibit low corrosion rates, on the order of  $1/_{10}$  to  $1/_{80}$  of the value exhibited by the black steel bars. However, five other specimens, MS-1, MS-2, MS-4, MS-5, and MS-8, exhibit high corrosion rates ( $15$  to  $35 \mu\text{m/yr}$ ), in some cases after an initial period of relatively low corrosion. The specimens exhibiting high corrosion rates also exhibited significant corrosion deposits in the vicinity of the epoxy coating at the end of the bar. To check these results, an additional set of six specimens, three black and three clad, were tested using specimens with ends that were protected by a cap filled with epoxy. As shown in Figs. 28 and 29, the black steel bars with the caps behaved in a manner similar to that of specimens MB-1 through MB-6, with corrosion rates fluctuating between  $15$  and  $35 \mu\text{m/yr}$  (Fig. 28). The stainless steel specimens, MSC-1 through MSC-3, exhibited corrosion rates between  $0$  and  $0.3 \mu\text{m/yr}$ , averaging about  $1/_{100}$  of the value observed for the black bars.

During most of the test period, the potentials of the anodes and cathodes in the macrocell

tests were measured. These results are presented in Appendix A in Figs. A.1-A.14. In macrocells with little corrosion, the potentials of the anode and cathode are nearly identical. In actively corroding macrocells, the potential of the anode is about 0.1 V below the potential of the cathode.

*Stage 2* – In Stage 2, the rapid corrosion potential and macrocell tests were repeated using steel bars embedded in mortar. These test specimens help provide a realistic appraisal of the tendency of the reinforcing bars to corrode in reinforced concrete.

The results of the **corrosion potential tests** are shown in Figs. 30-33. Although highly variable, the corrosion potential tests of the black steel bars embedded in mortar (Figs. 30 and 31) exhibit corrosion potentials between  $-0.3$  and  $-0.6$  V. The results indicate that not one of the six specimens was passive and that all six exhibited a tendency to corrode.

The results for the stainless steel clad specimens (Figs. 32 and 33) indicate that only one out of the six specimens did not passivate during the 40-day period. An inspection of this specimen following the tests indicated that corrosion occurred at the upper portion of the metal near the epoxy ring (Fig. 1), perhaps due to migration of the salt solution through the concrete and under the epoxy.

The results for the **macrocell tests** are shown in Figs. 34-38. The macrocells for the black steel bars (Figs. 34 and 35 and specimen MBMS-1 in Fig. 38) exhibited corrosion rates between 2 and 5  $\mu\text{m}/\text{yr}$ . These values are considerably less than that exhibited by the bars without mortar, but match the values obtained in earlier research for specimens embedded in mortar (Darwin 1995, Senecal et al. 1995, Schwensen et al. 1995). Stainless steel clad bars embedded in mortar (Figs. 36 and 37 and specimen MSMS-1 in Fig. 38) exhibited corrosion rates between 0 and 0.2  $\mu\text{m}/\text{yr}$  with an average value of about 0.1  $\mu\text{m}/\text{yr}$ ,  $1/20$  to  $1/50$  of the value exhibited by the black steel.

Anode and cathode corrosion potential measurements for the macrocell test specimens embedded in mortar are presented in Appendix A in Figs. A.15-A.24.

## DISCUSSION AND RECOMMENDATIONS

The specimens evaluated in this study represent prototype bars. The variation in the thickness of the cladding and the formation of the indent and its associated crack may present problems if not corrected in full-scale production. Considering an average corrosion rate of about 0.2  $\mu\text{m}/\text{yr}$  for stainless steel bars with caps and not embedded in mortar (representing a corrosion rate that might be expected at a void adjacent to the bar in concrete), the current cladding thickness appears to be satisfactory if the current minimum thickness of 0.196 mm (7.7 mils) is maintained.

The stainless steel clad bars exhibit about two orders of magnitude less corrosion than black reinforcement, indicating that the material offers significant potential for reinforced concrete structures subjected to severe corrosion conditions. A principal area of concern, however, is the need to ensure that the mild steel core does not come in contact with chlorides, as indicated in the Stage 1 tests. On those specimens in which the epoxy coating was breached and corrosion occurred, the clad reinforcement behaved similar to the black steel. Thus, well-protected ends and procedures to ensure that the cladding is not breached at locations along the bar should receive the highest attention. It is recommended that, if the current system is used, the end protection procedures, caps filled with epoxy or other techniques, be marketed along with the steel to ensure that the system maintains its integrity.

Along that line, it is recommended that SMI consider the use of 316 stainless steel. This recommendation is based on work by McDonald et al. (1998), which included a comparison of the corrosion performance of solid 304 and 316 stainless steel bars. Under conditions in which the stainless steel acted as both the anode and the cathode, the 304 stainless steel was about twice as corrosion resistant as the 316 stainless steel. However, in cracked concrete, when mixed with black steel, the corrosion rate of the 304 stainless steel increased by 50 times, while the 316 stainless steel exhibited little change in corrosion performance. This indicates that the use of 316 cladding may prove to be superior to 304 cladding. For that reason, corrosion tests of 316 stainless steel clad reinforcement are recommended.

It is also recommended that SMI carry out longer-term tests, such as Southern Exposure tests (Darwin 1995, Senecal et al. 1995, McDonald et al. 1998), including combinations with black steel, to fully evaluate the performance of the clad reinforcement. Combinations with black steel are important because designers often use conventional reinforcing bars in portions of structures which they do not expect to be subjected to chloride attack.

## CONCLUSIONS

The following conclusions are based on the tests and analyses presented in this report.

1. The stainless steel cladding provides significant corrosion protection if it is fully intact.
2. Corrosion rates for clad bars not encased in mortar range from 0 to 0.3  $\mu\text{m}/\text{yr}$ , averaging about  $1/100$  of the value observed for black bars. Clad bars embedded in mortar exhibit corrosion rates between 0 and 0.2  $\mu\text{m}/\text{yr}$ , averaging  $1/20$  to  $1/50$  of the value exhibited by black bars embedded in mortar.
3. If the cut ends of the bars are not protected so that the mild steel core is isolated from chlorides, the clad bars corrode at approximately the same rate as black steel bars.
4. The cladding thickness varies significantly around the periphery of the bar. The most significant variation involves the formation of an indent of cladding at the longitudinal rib. Longitudinal cracks are centered on the indent. The cracks do not penetrate the cladding, but may represent a potential problem in production bars. At one location a crack between the mild steel and the cladding was observed at the indent.

It is recommended: (a) that SMI evaluate 316 stainless steel in addition to 304 stainless steel as a cladding material, (b) that the bars be subjected to longer-term tests, and (c) that, if the

current system is used, end protection procedures be marketed along with the steel to insure that the system maintains its integrity.

### ACKNOWLEDGEMENTS

This study was supported by Structural Metals, Inc. and the Department of Civil and Environmental Engineering at the University of Kansas. Figures 1 - 3 were drafted by Robert Zechmann.

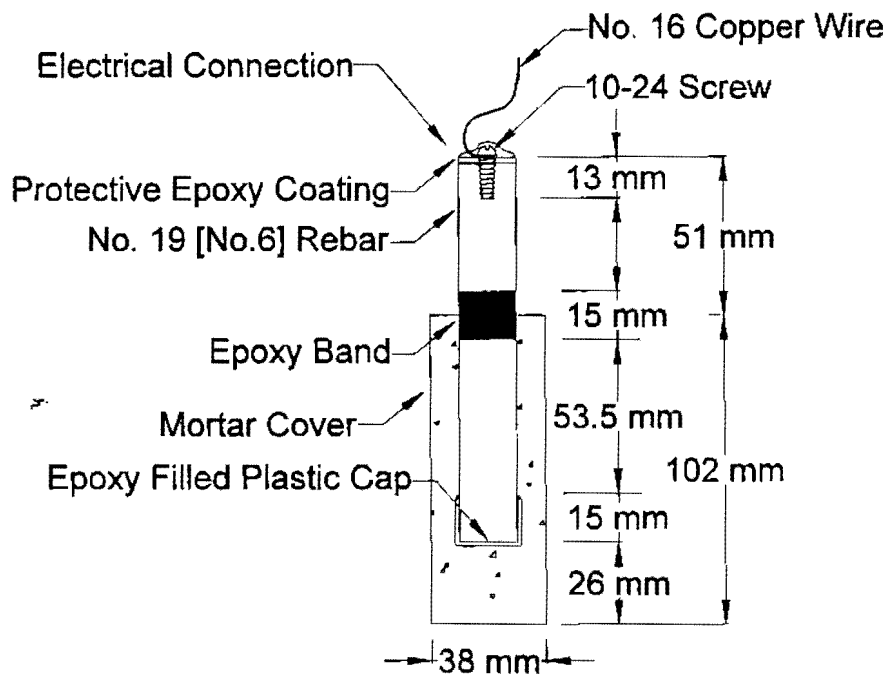
### REFERENCES

- Darwin, D., 1995. "Corrosion-Resistant Steel Reinforcing Bars, Summary Report," *SL Report* 95-2, University of Kansas Center for Research, Inc., Lawrence, Kansas, May, 22 pp.
- Farzammehr, H., 1985. "Pore Solution Analysis of Sodium and Calcium Chloride Containing Cement Pastes," *Master of Science Thesis*, University of Oklahoma, Norman, OK.
- McDonald, D. B., Pfeifer, D. W., and Sherman, M. R. 1998. "Corrosion Evaluation of Epoxy-Coated, Metallic-Clad and Solid Metallic Reinforcing Bars in Concrete," *Publication* No. FHWA-RD-98-153, Federal Highway Administration, McLean, VA, Dec., 127 pp.
- Schwensen, S. M., Darwin, D., and Locke, C. E., Jr., 1995. "Rapid Evaluation of Corrosion-Resistant Concrete Reinforcing Steel in the Presence of Deicers," *SL Report* 95-6, University of Kansas Center for Research, Inc., Lawrence, Kansas, July, 90 pp.
- Senecal, M. R., Darwin, D., and Locke, C. E., Jr., 1995. "Evaluation of Corrosion-Resistant Steel Reinforcing Bars," *SM Report* No. 40, University of Kansas Center for Research, Inc., Lawrence, Kansas, July, 142 pp.

**Table 1 - Variation in cladding thickness for transversely cut specimens**

<b>Specimen</b>	<b>Minimum (mm)</b>	<b>Maximum (mm)</b>	<b>Mean (mm)</b>
1	0.196	0.844	0.488
2	0.301	0.894	0.524
3	0.226	0.864	0.453
4	0.245	0.750	0.445
5	0.243	0.726	0.442
6	0.255	0.735	0.450
<b>Total</b>	0.196	0.894	0.467

1 mm = 0.0394 in. = 39.4 mils

**Figure 1 - Cross Section of Mortar Specimen**



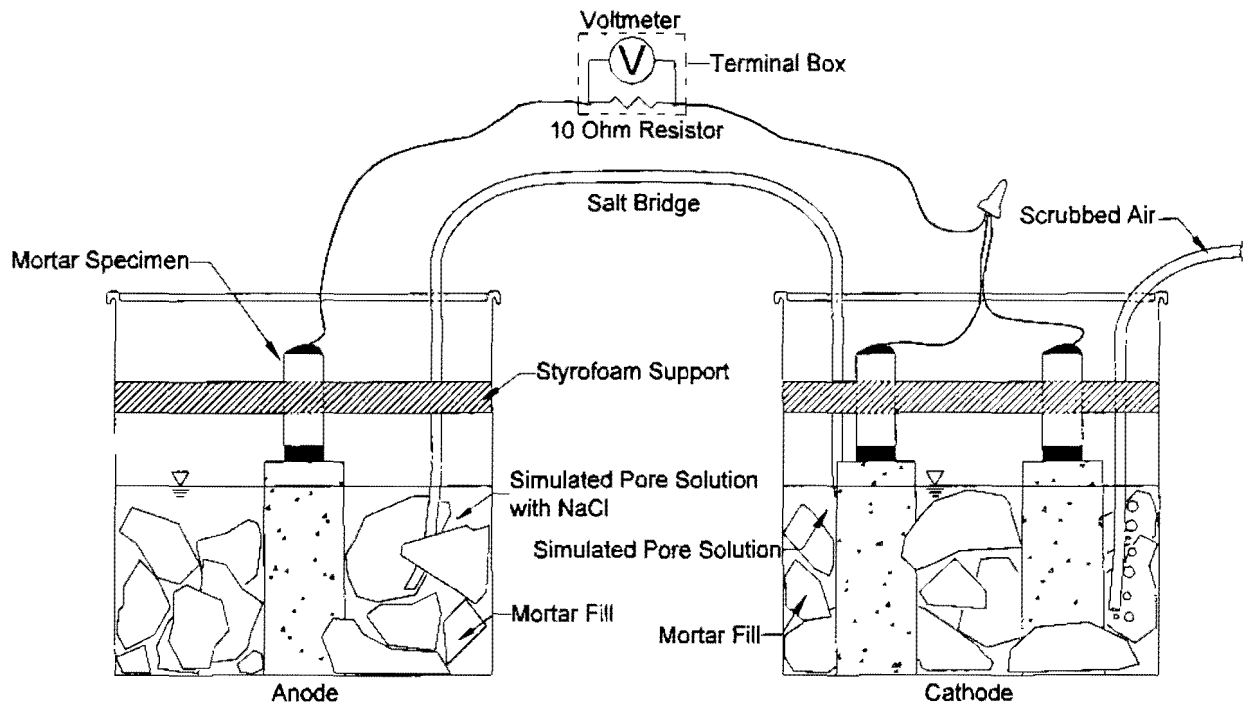


**Figure 2 - Schematic of Macroc cell Corrosion Test**

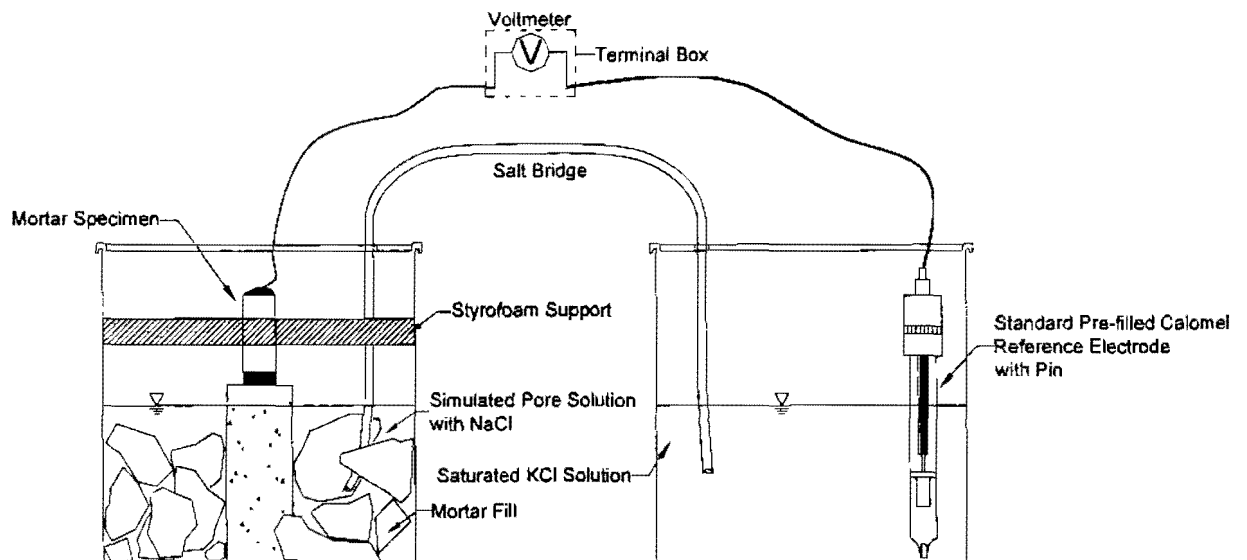


**Figure 3 - Schematic of Corrosion Potential Test**

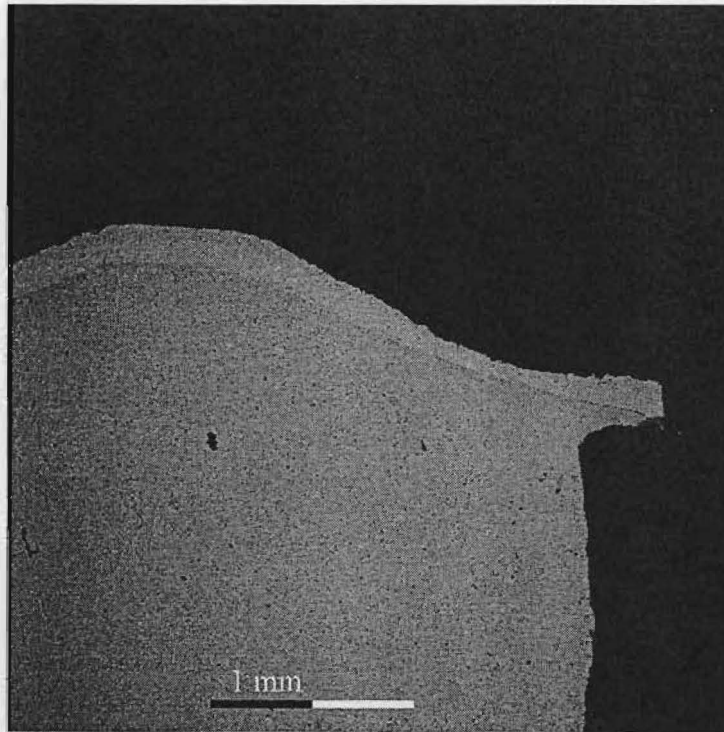


**Figure 4** - Variation in stainless steel cladding thickness for longitudinally cut specimen

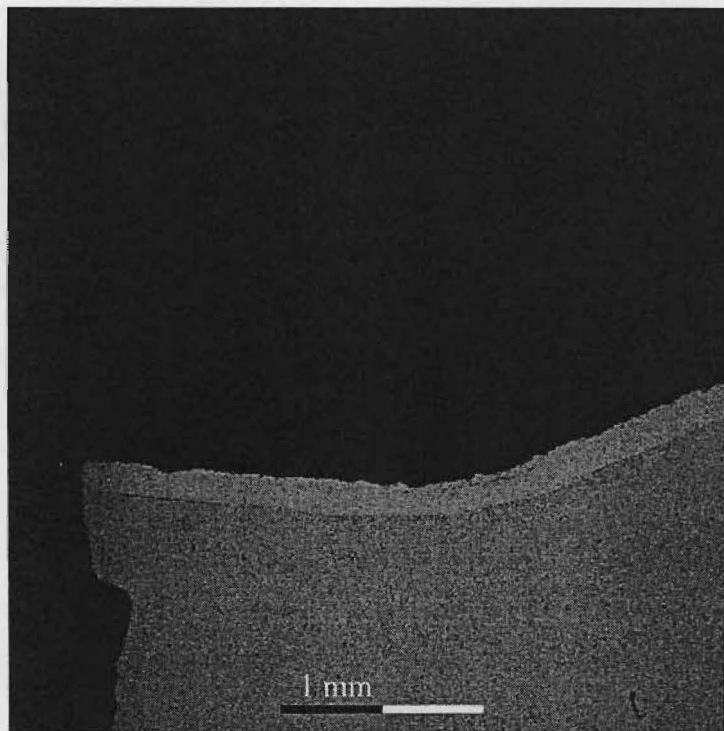


**Figure 5** - Variation in stainless steel cladding thickness for the left side of the specimen shown in Figure 4

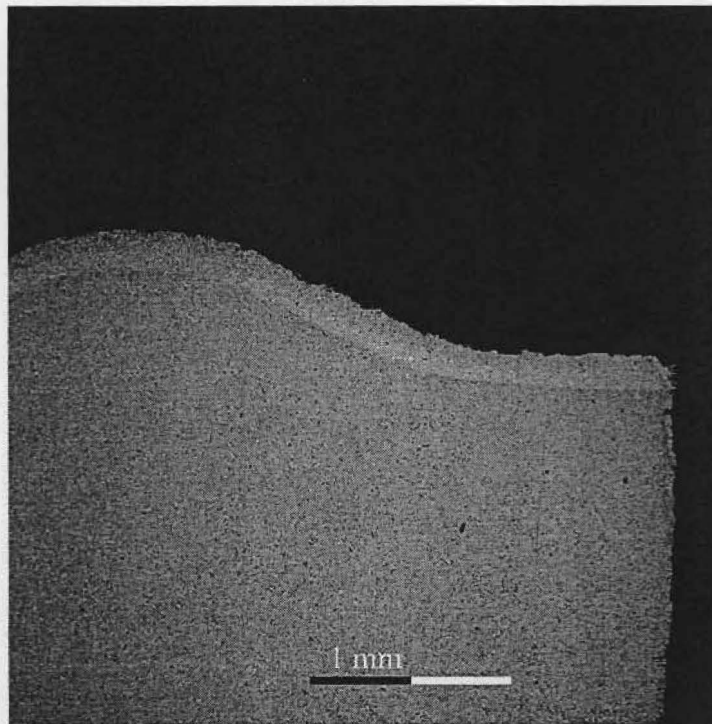


**Figure 6** - Variation in stainless steel cladding thickness for longitudinally cut specimen

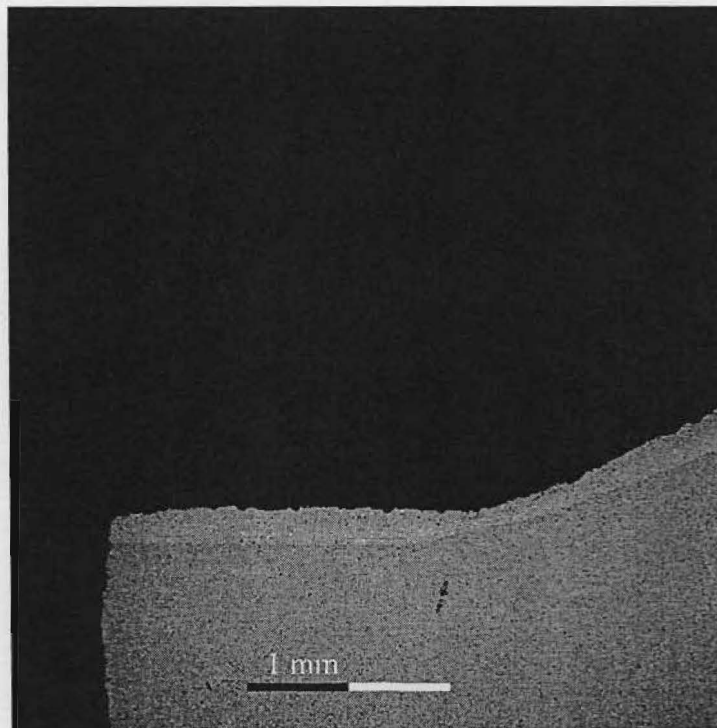


**Figure 7** - Variation in stainless steel cladding thickness for the left side of the specimen shown in Figure 6

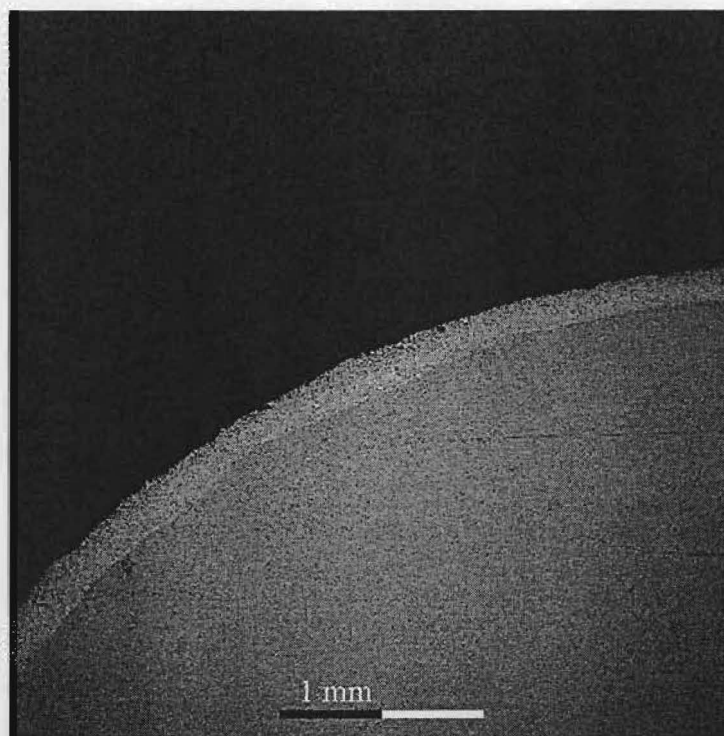


**Figure 8** - Variation in stainless steel cladding thickness for transversely cut specimen

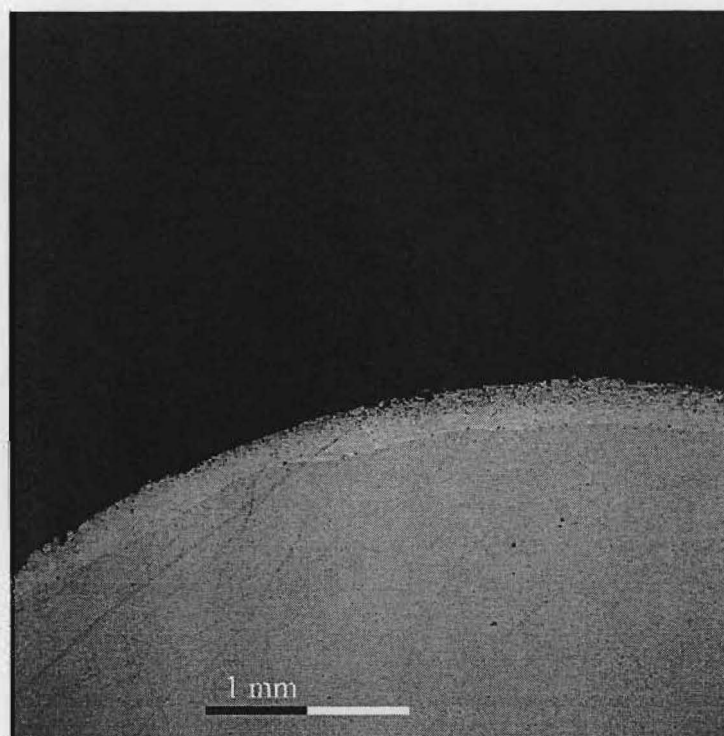


**Figure 9** - Variation in stainless steel cladding thickness for transversely cut specimen

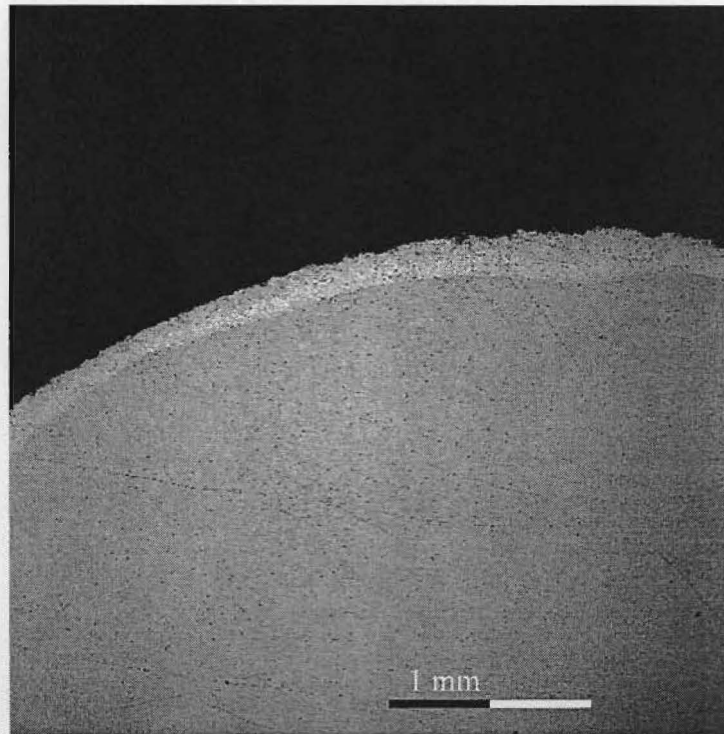


**Figure 10** - Variation in stainless steel cladding thickness for transversely cut specimen

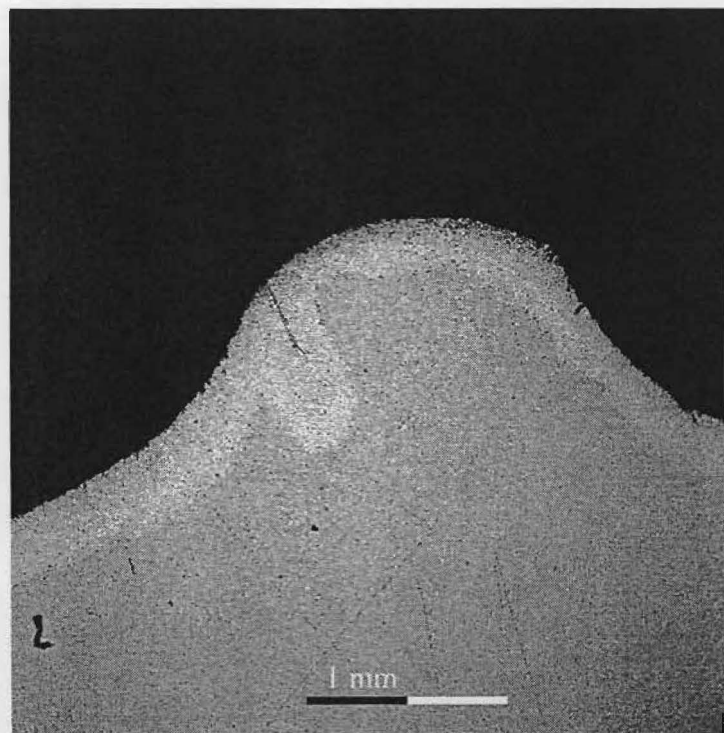


**Figure 11** - Crack in stainless steel indentation at longitudinal rib



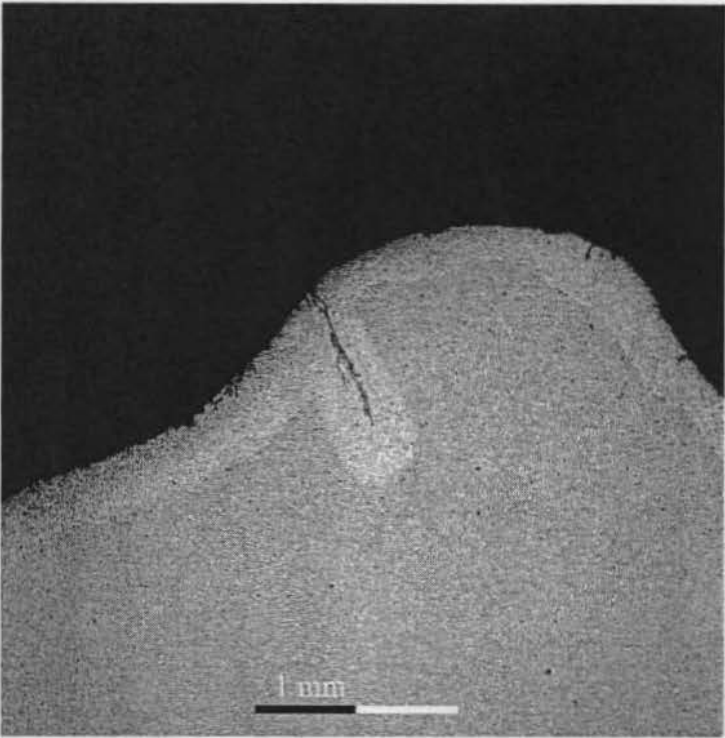


**Figure 12** - Crack in stainless steel indentation at longitudinal rib

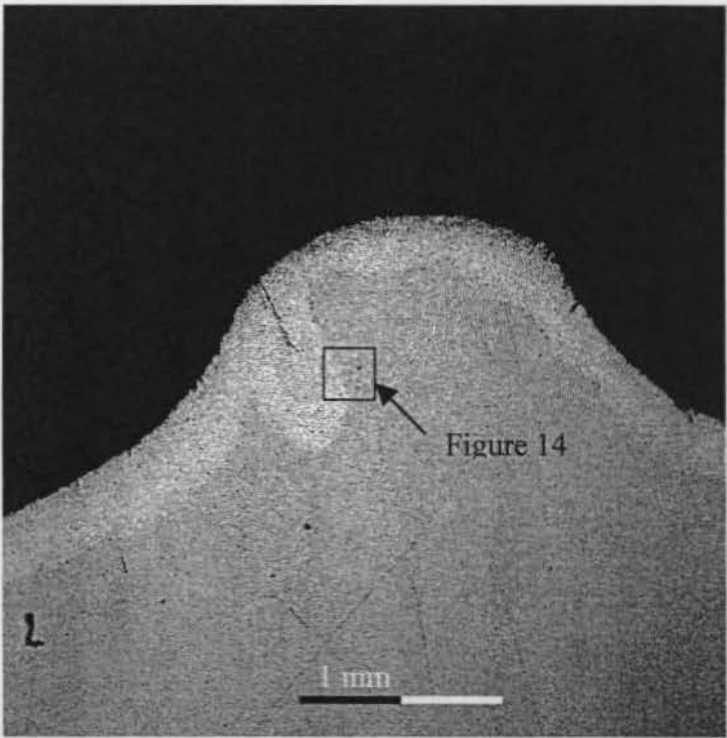


**Figure 13** - Crack in stainless steel indentation at longitudinal rib

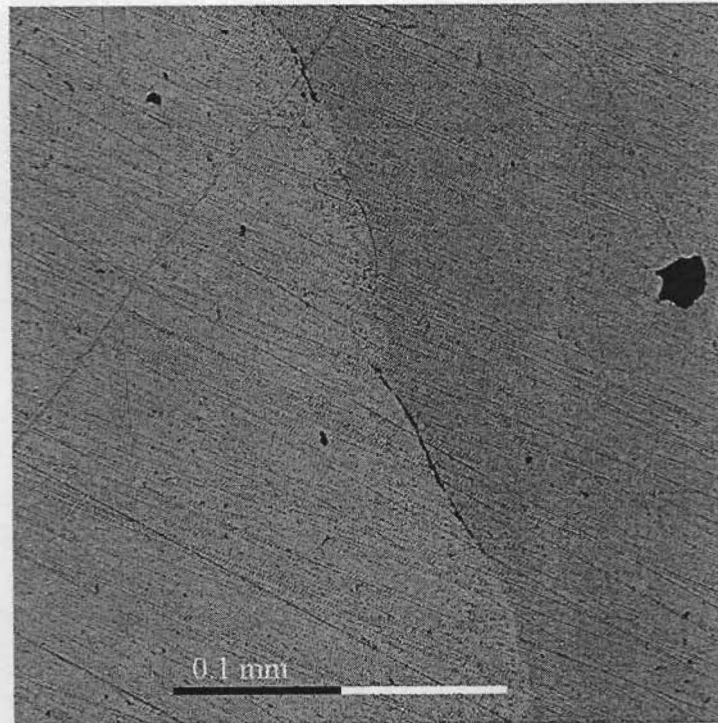


**Figure 14** - Crack along interface between stainless steel cladding (at indentation) and mild steel. Region is shown in Figure 13. Crack thickness is approximately 1.5  $\mu\text{m}$ .

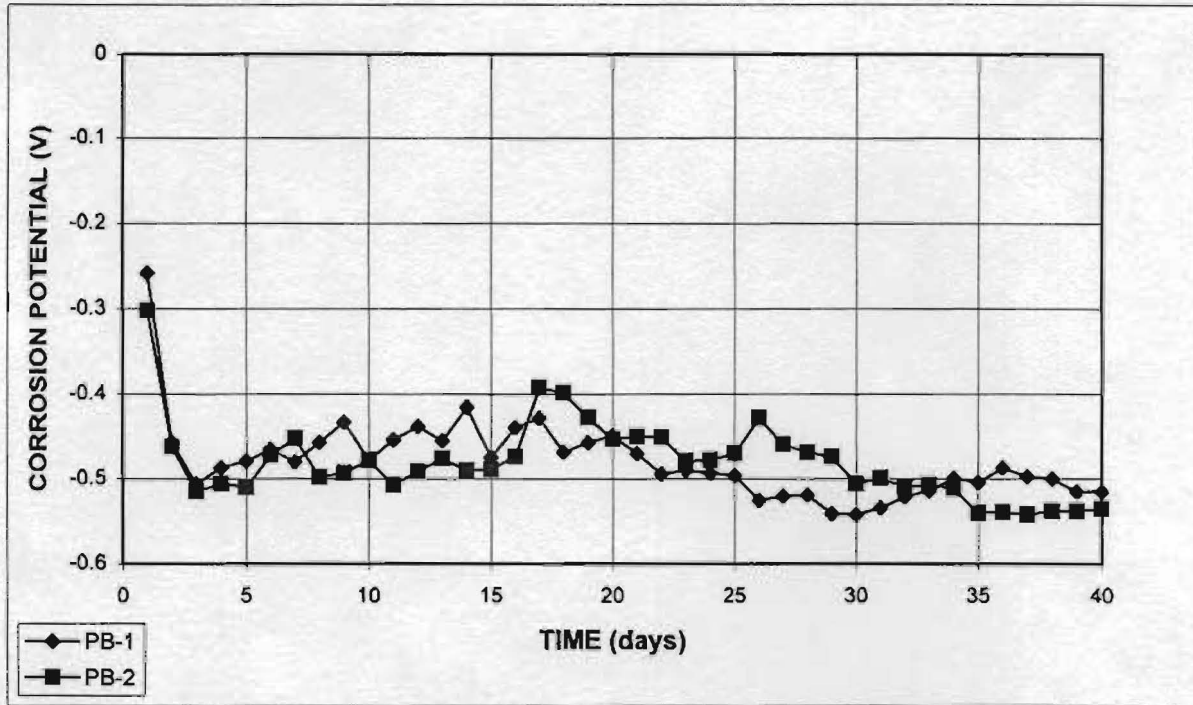


Figure 15 - Corrosion Potential Test: Black steel without mortar. Specimens PB-1 and PB-2

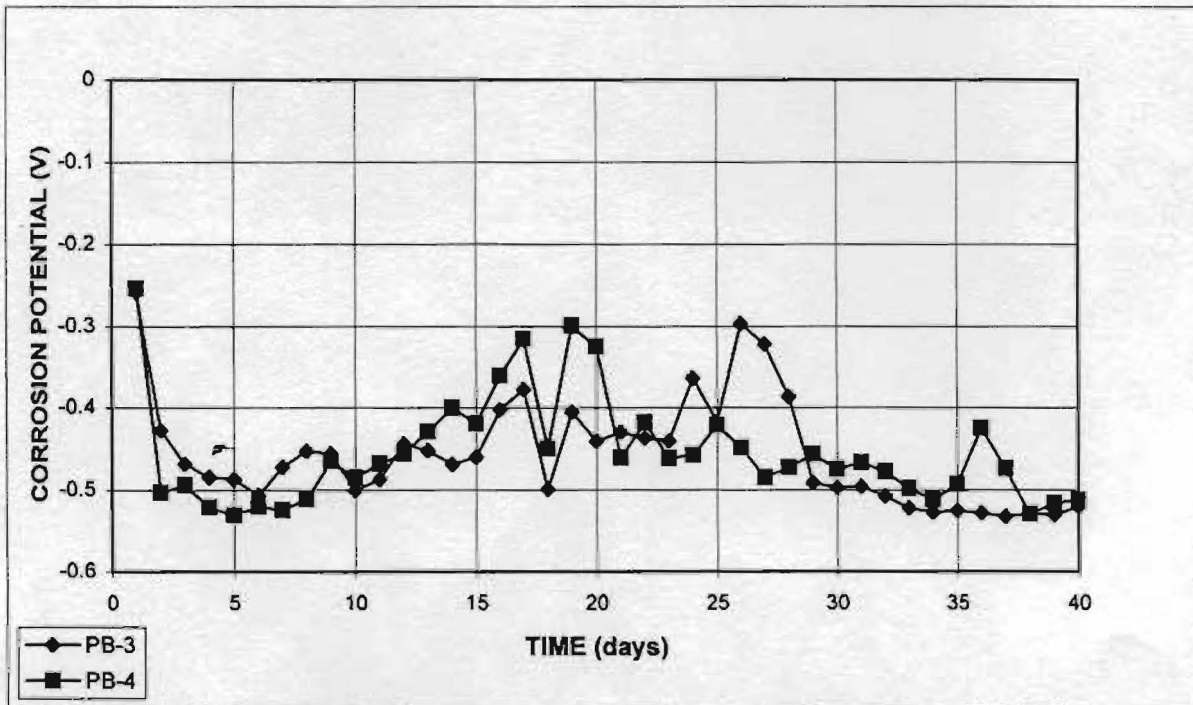


Figure 16 - Corrosion Potential Test: Black steel without mortar. Specimens PB-3 and PB-4



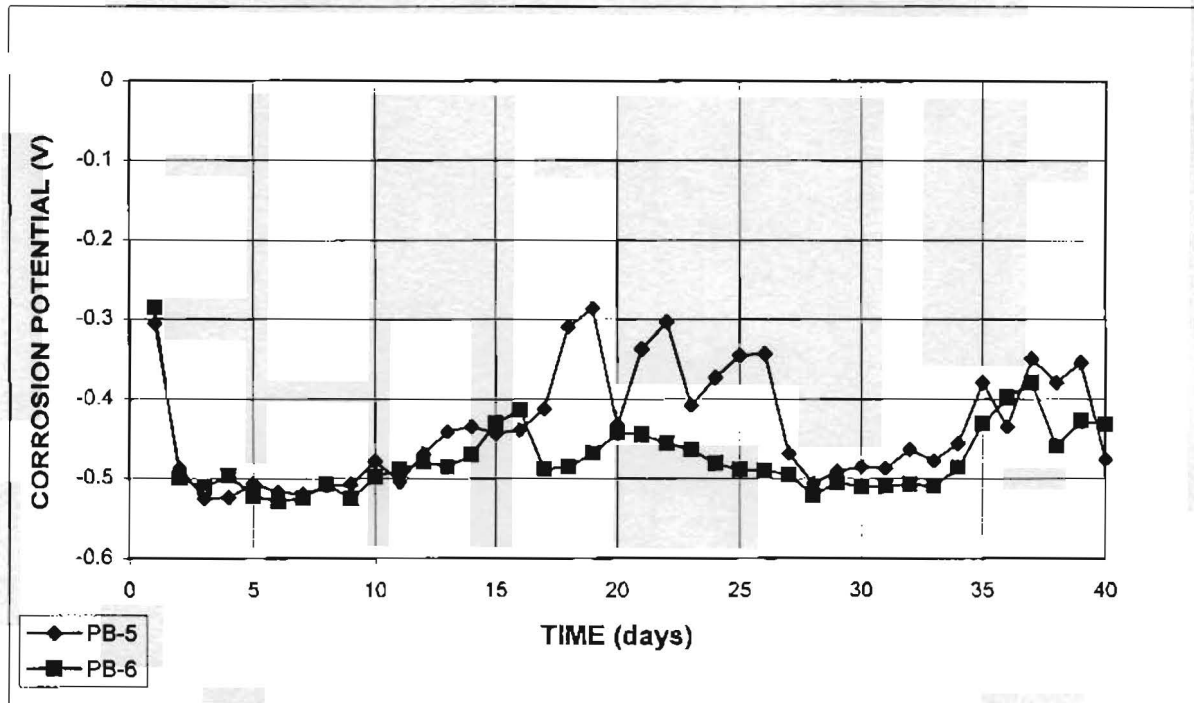


Figure 17 - Corrosion Potential Test: Black steel without mortar. Specimens PB-5 and PB-6

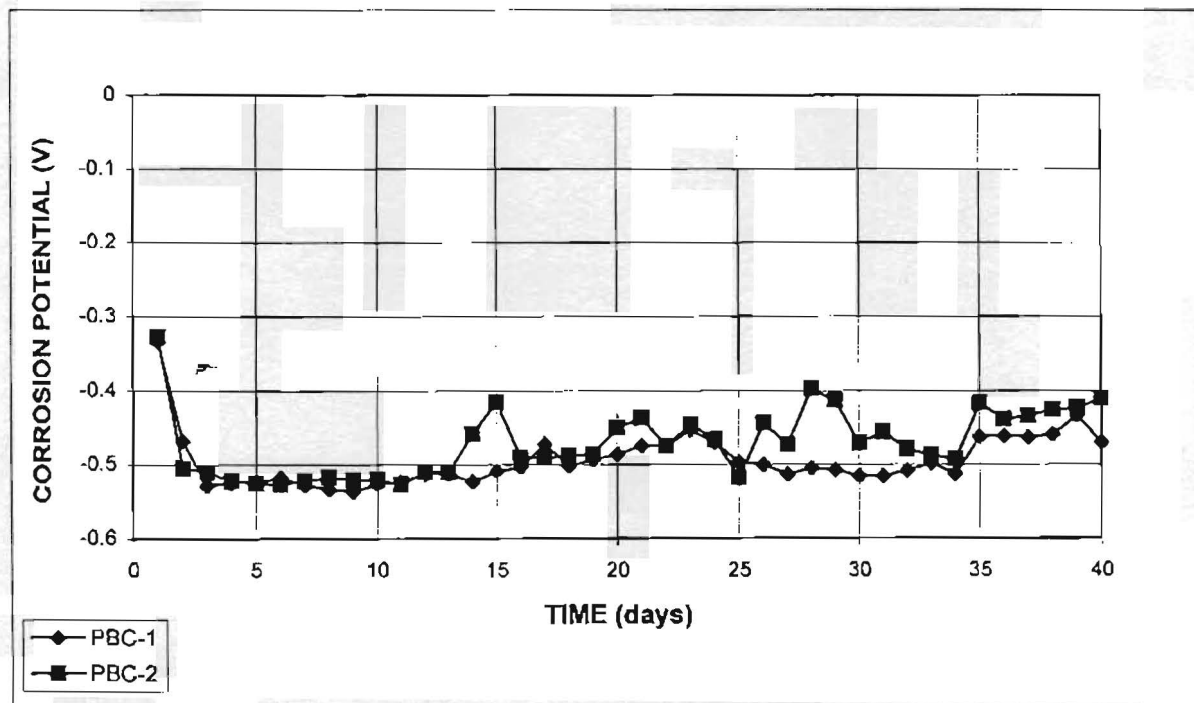


Figure 18 - Corrosion Potential Test: Black steel without mortar, with caps. Specimens PBC-1 and PBC-2

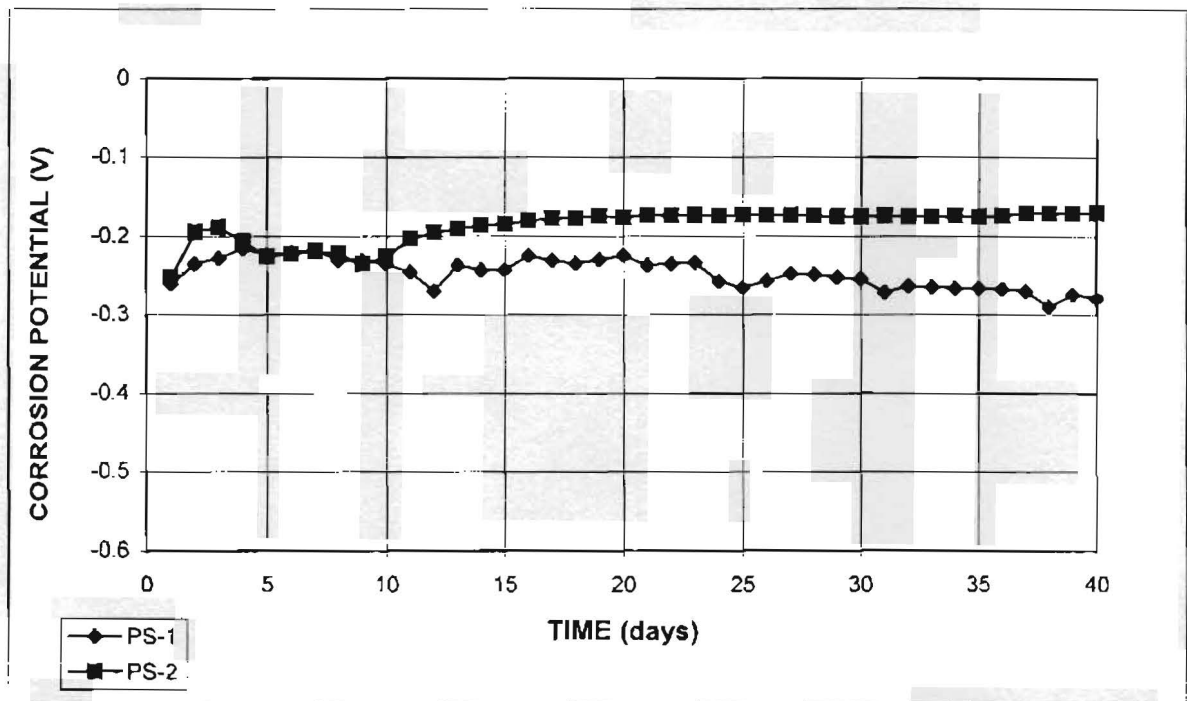


Figure 19 - Corrosion Potential Test: Stainless steel clad without mortar. Specimens PS-1 and PS-2

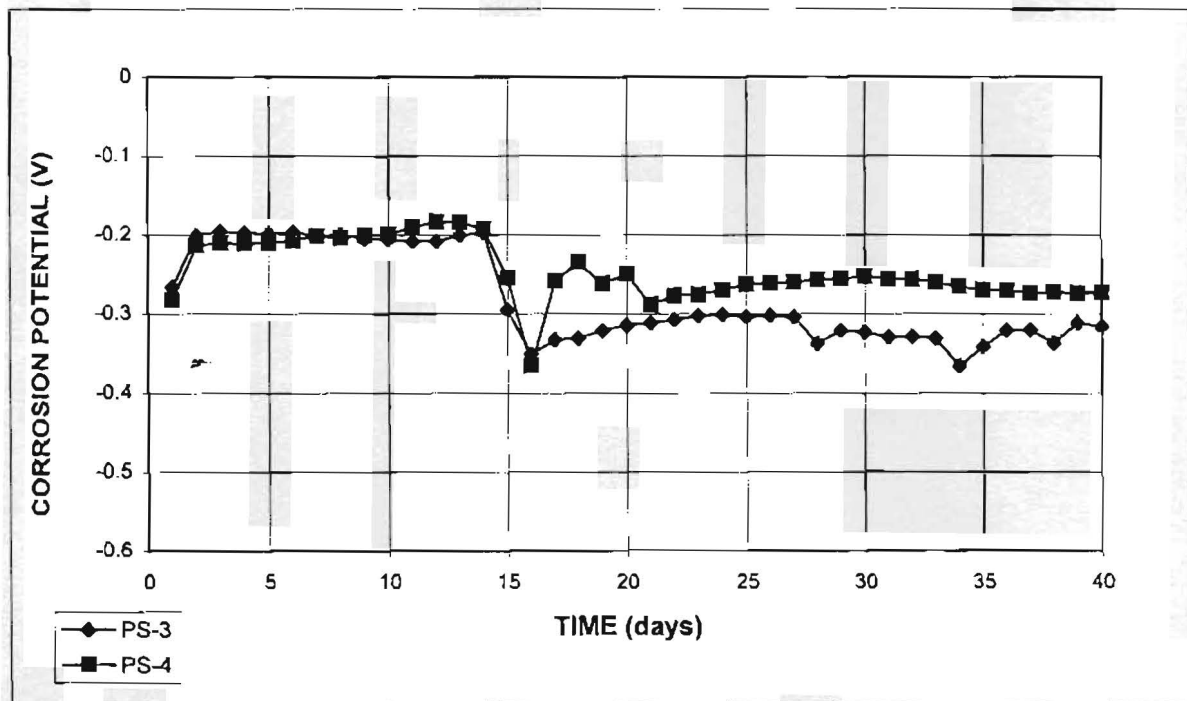


Figure 20 - Corrosion Potential Test: Stainless steel clad without mortar. Specimens PS-3 and PS-4

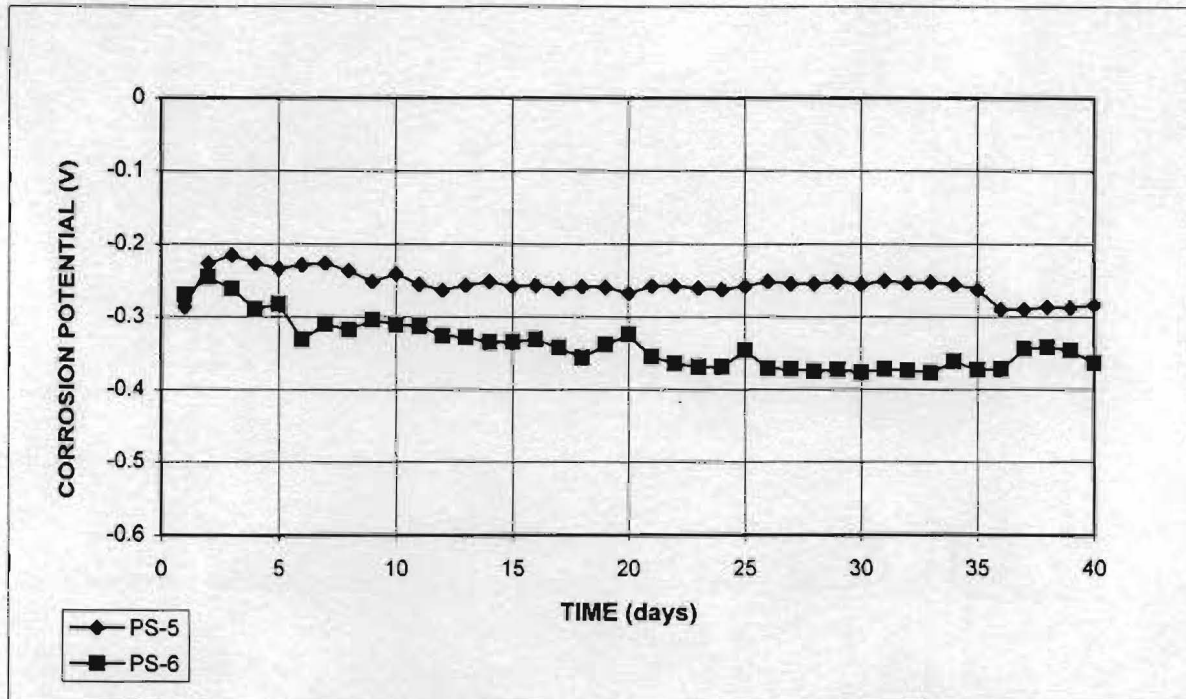


Figure 21 - Corrosion Potential Test: Stainless steel clad without mortar. Specimens PS-5 and PS-6

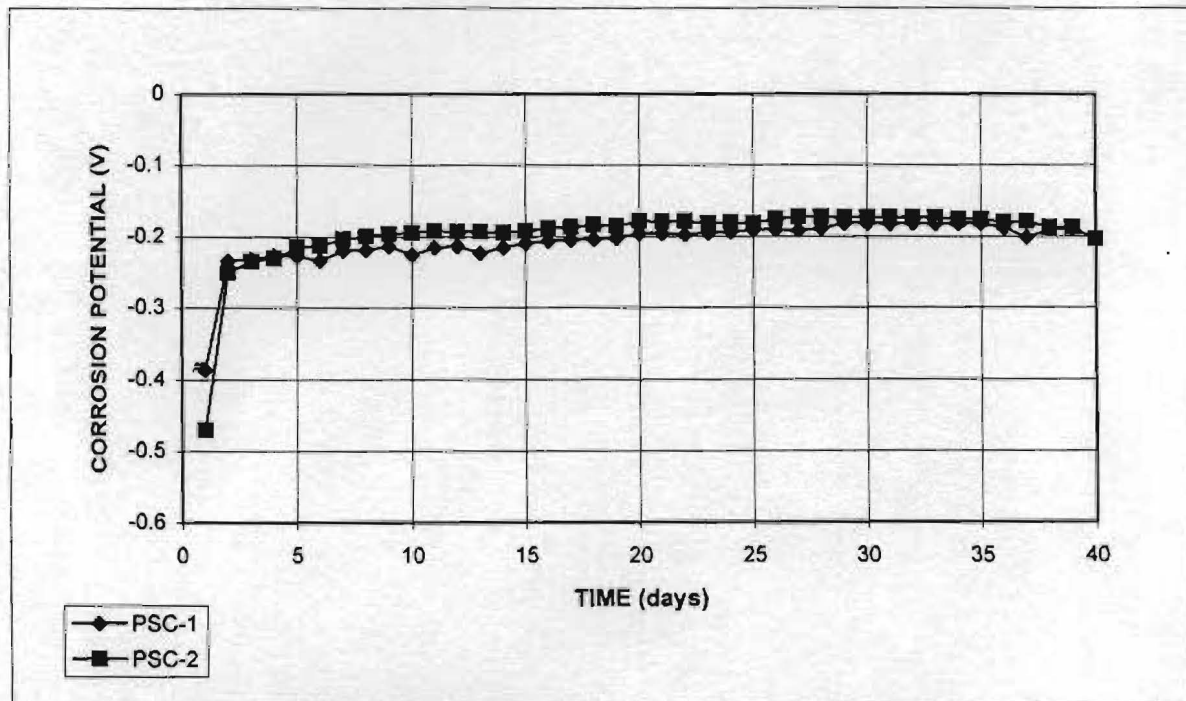


Figure 22 - Corrosion Potential Test: Stainless steel clad without mortar, with caps. Specimens PSC-1 and PSC-2.

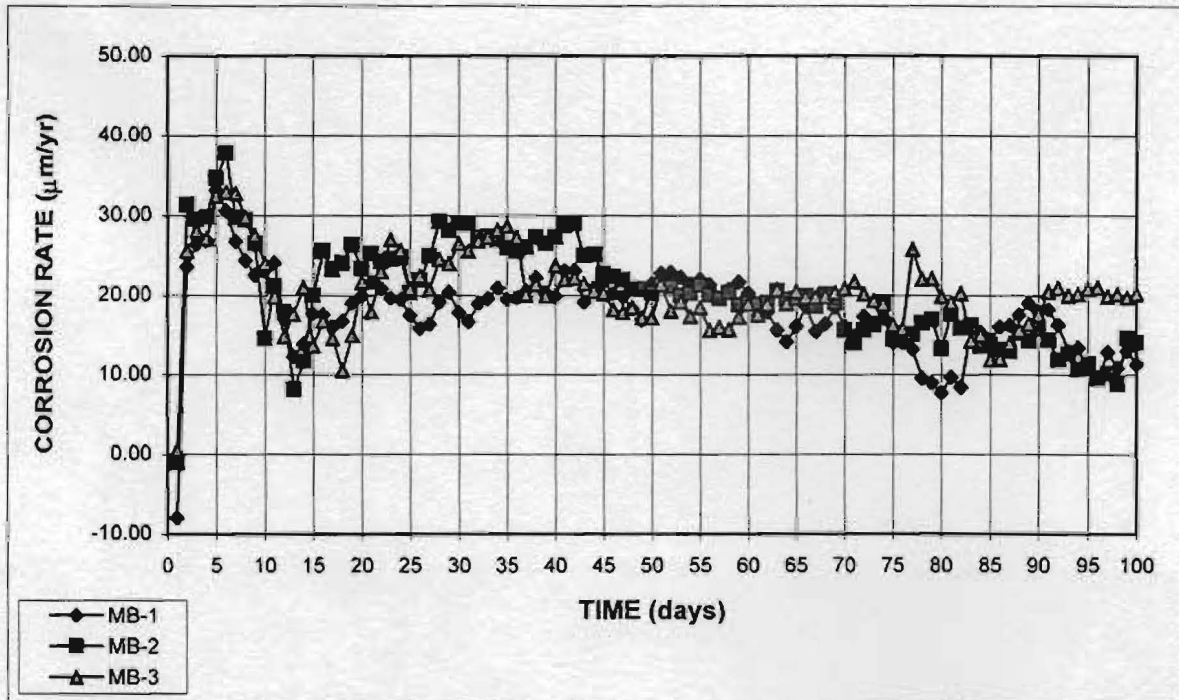


Figure 23 - Macrocell Test: Black steel without mortar. Specimens MB-1, MB-2 and MB-3

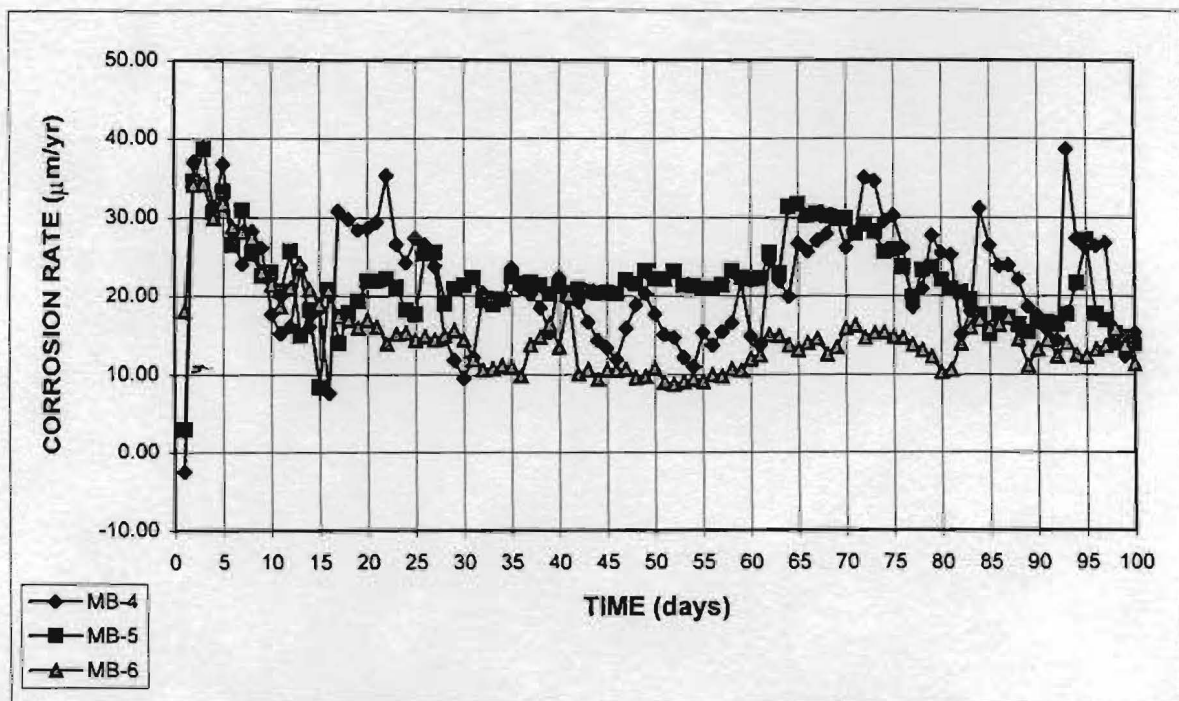


Figure 24 - Macrocell Test: Black steel without mortar. Specimens MB-4, MB-5 and MB-6

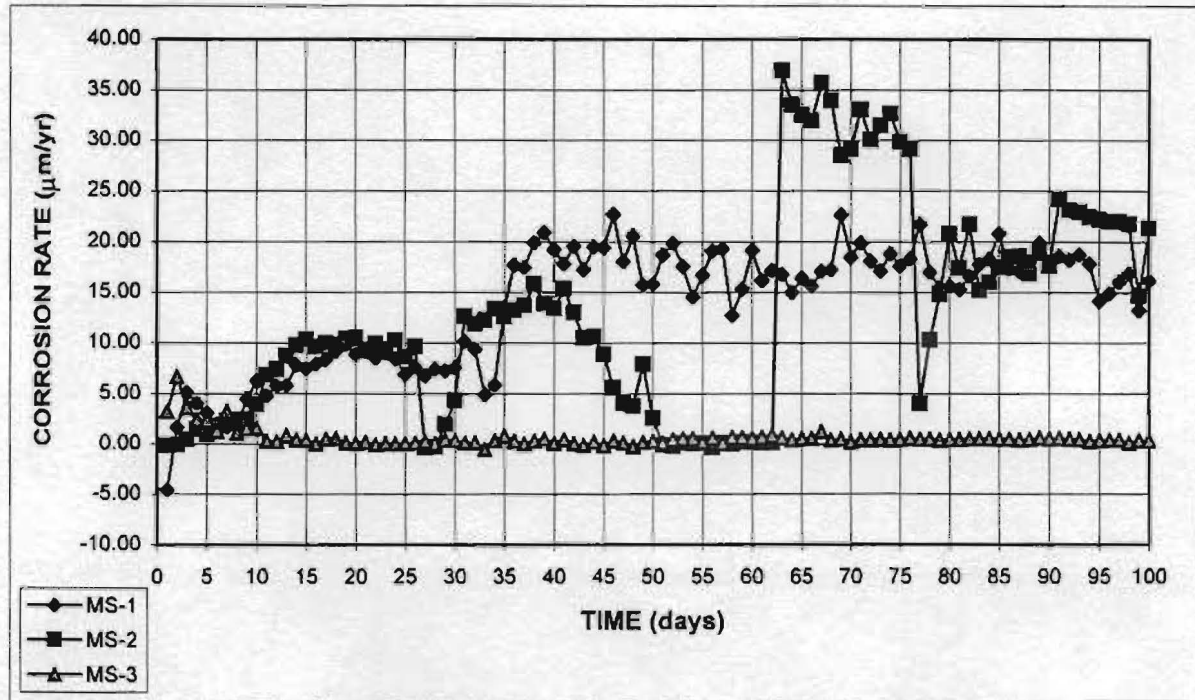


Figure 25a - Macroc cell Test: Stainless steel clad without mortar. Specimens MS-1, MS-2 and MS-3

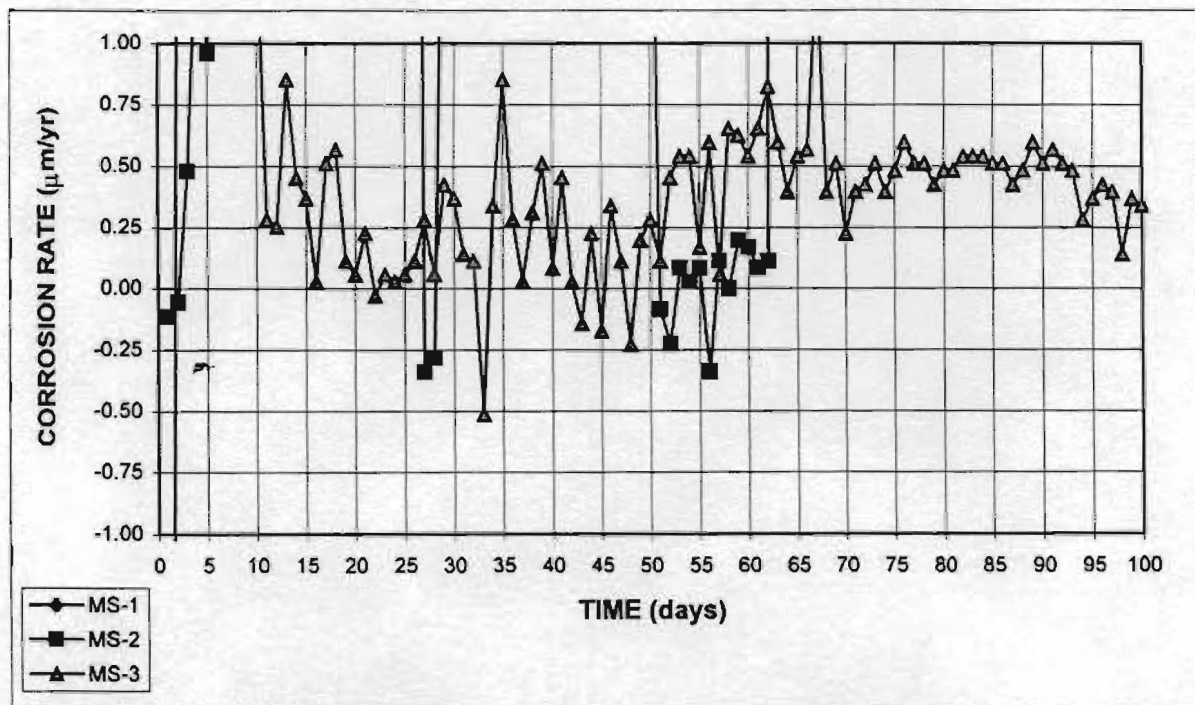


Figure 25b - Macroc cell Test: Stainless steel clad without mortar. Specimens MS-1, MS-2 and MS-3



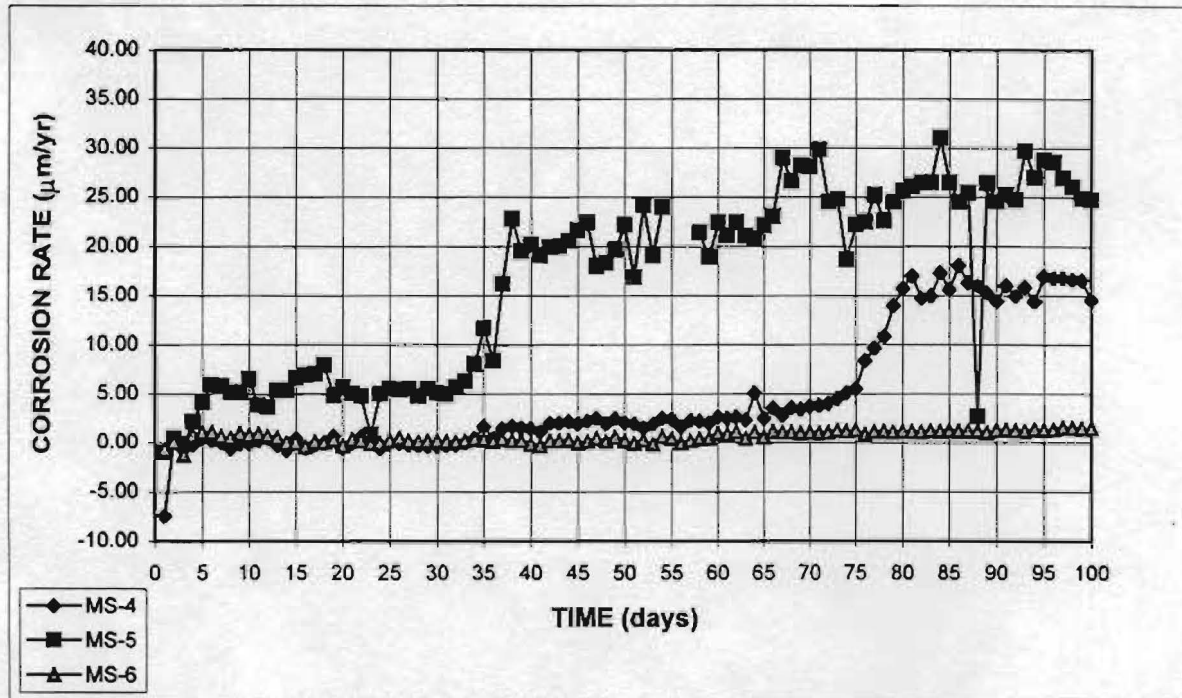


Figure 26a - Macrocell Test: Stainless steel clad without mortar. Specimens MS-4, MS-5 and MS-6

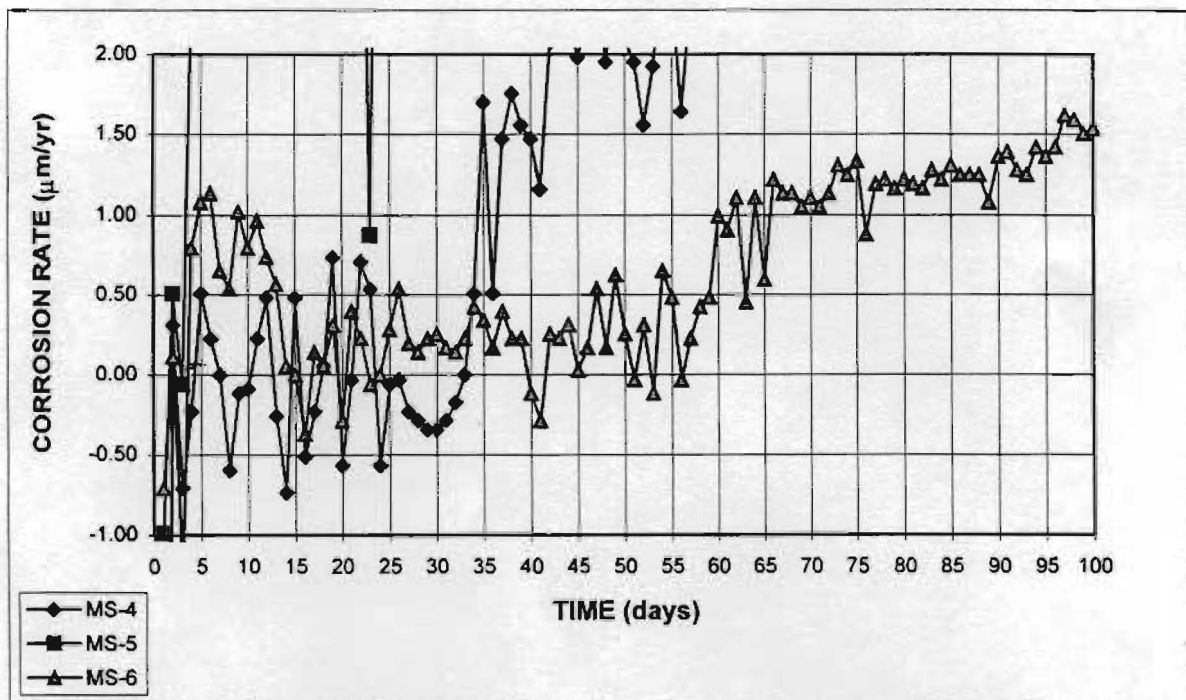


Figure 26b - Macrocell Test: Stainless steel clad without mortar. Specimens MS-4, MS-5 and MS-6

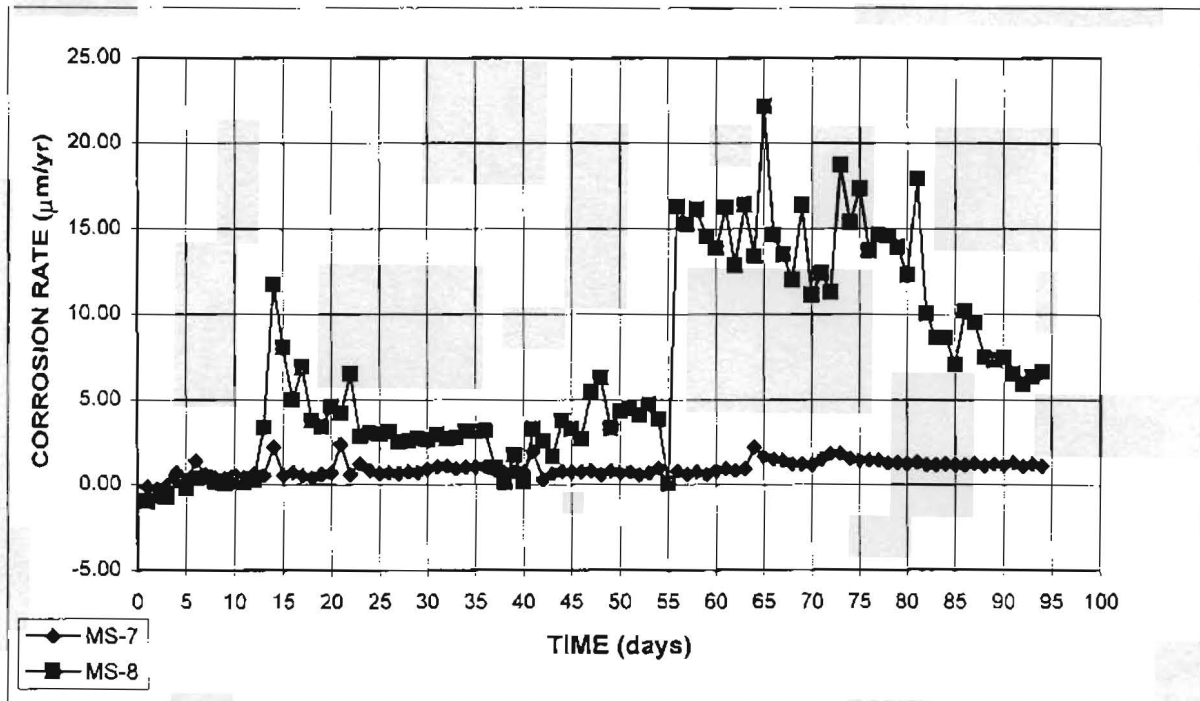


Figure 27a - Macrocell Test: Stainless steel clad without mortar. Specimens MS-7 and MS-8

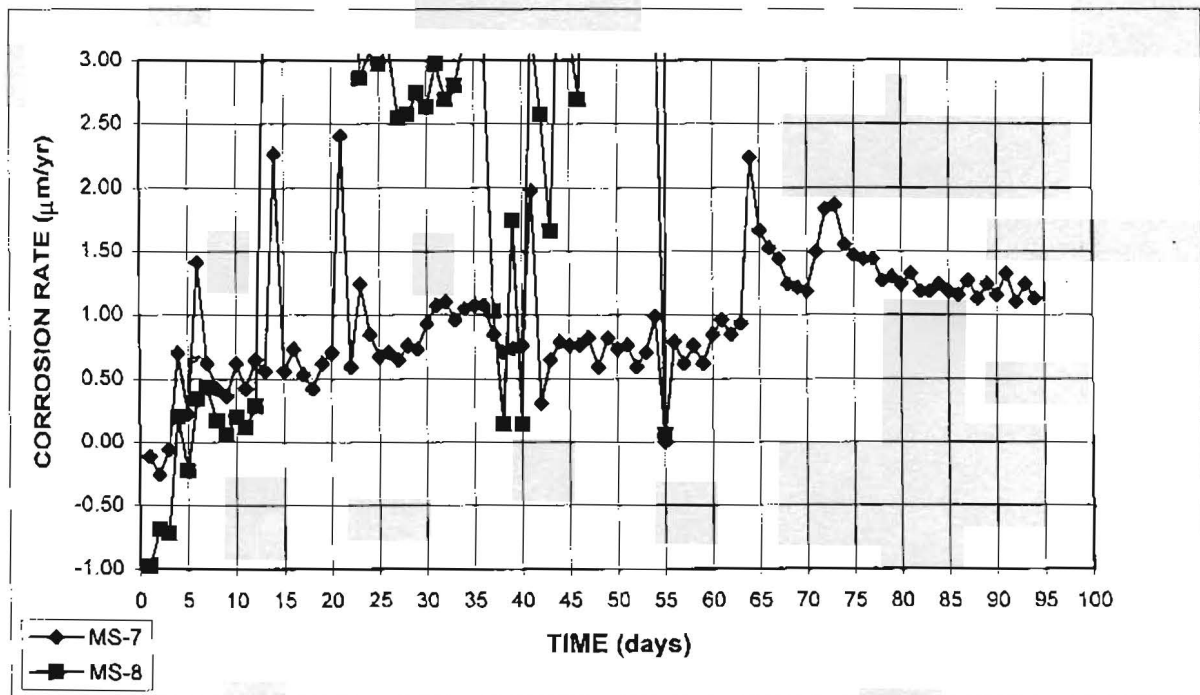


Figure 27b - Macrocell Test: Stainless steel clad without mortar. Specimens MS-7 and MS-8

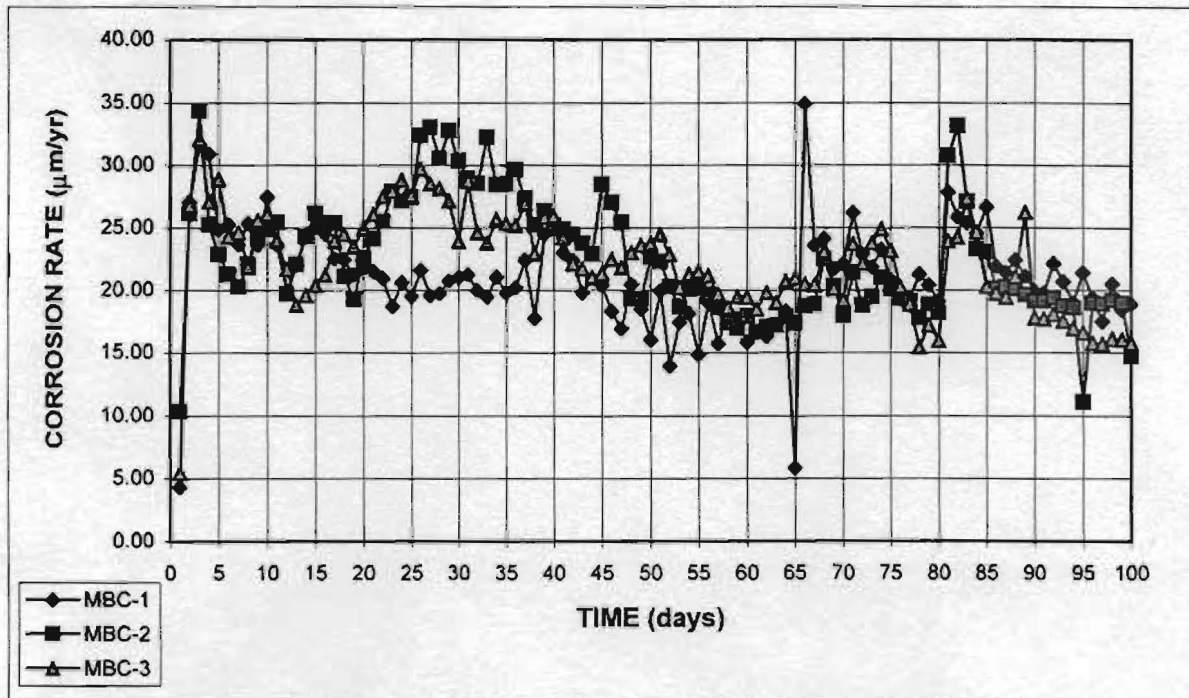


Figure 28 - Macrocell Test: Black bars without mortar, with caps.  
Specimens MBC-1, MBC-2 and MBC-3

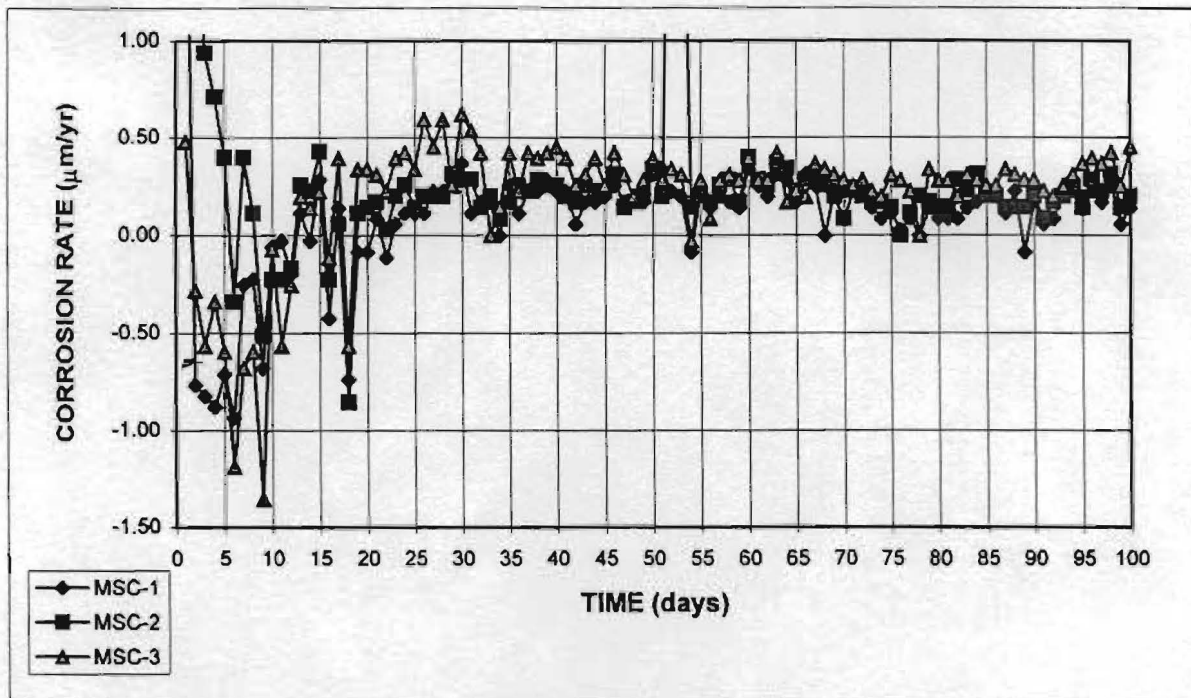


Figure 29 - Macrocell Test: Stainless steel clad bars without mortar, with caps.  
Specimens MSC-1, MSC-2 and MSC-3



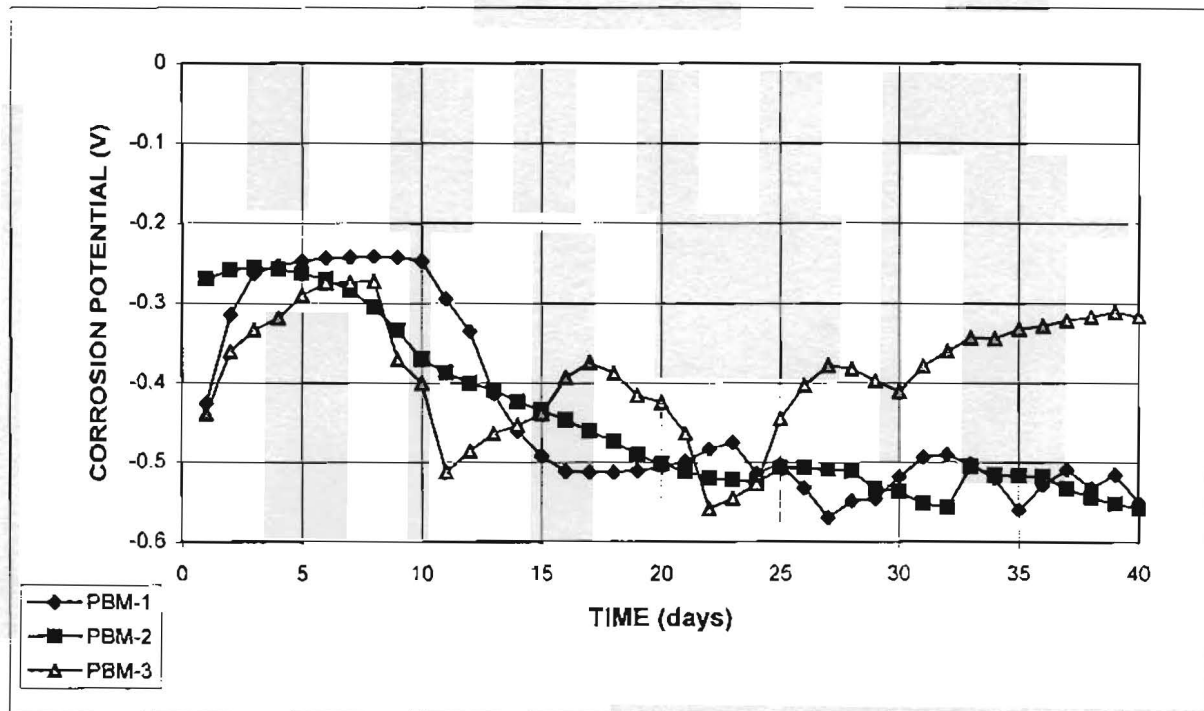


Figure 30 - Corrosion Potential Test: Black steel with mortar  
Specimens PBM-1, PBM-2, PBM-3

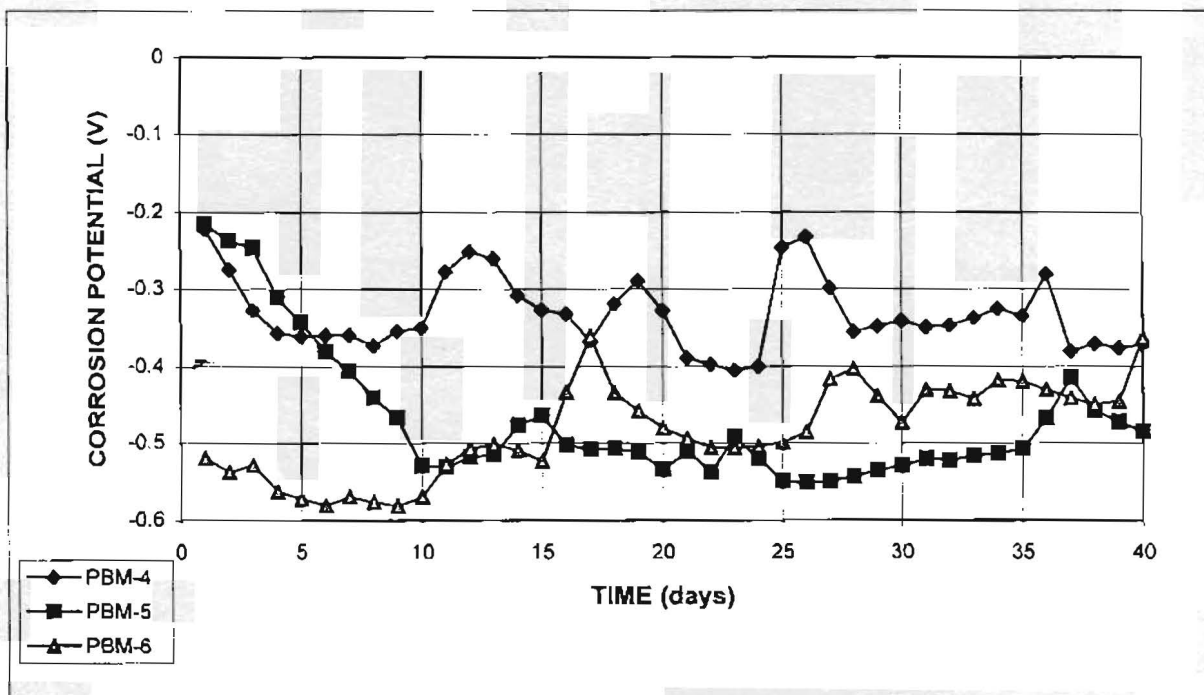


Figure 31 - Corrosion Potential Test: Black steel with mortar  
Specimens PBM-4, PBM-5, PBM-6

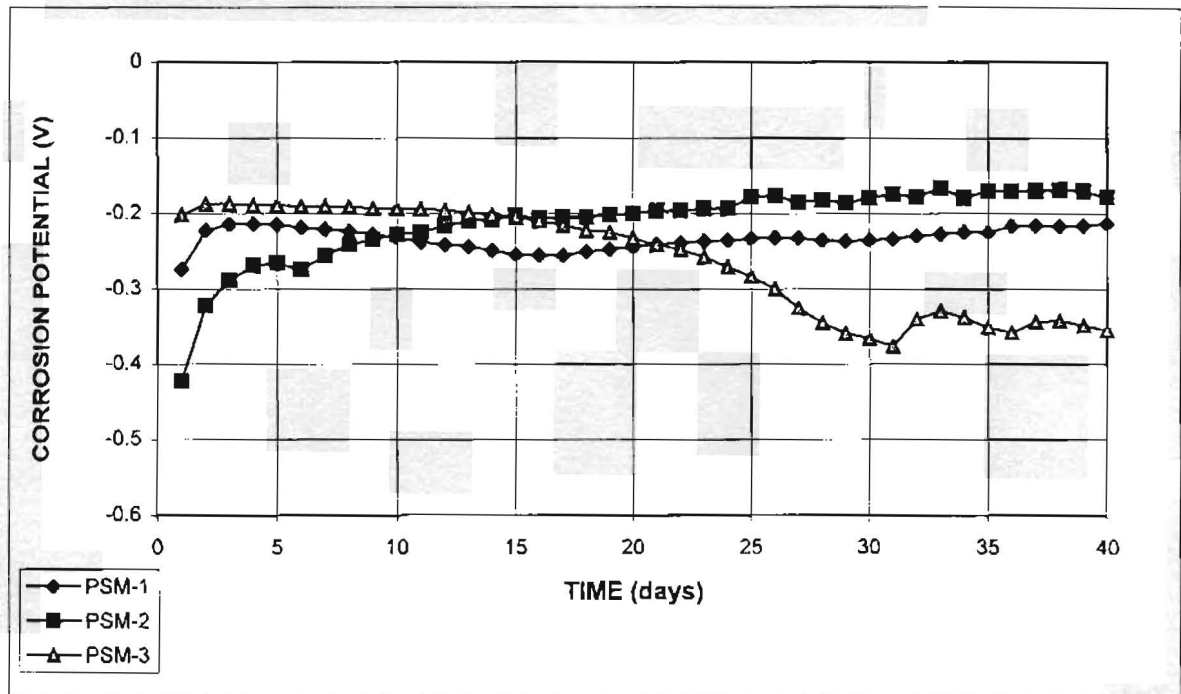


Figure 32 - Corrosion Potential Test: Stainless steel clad with mortar  
Specimens PSM-1, PSM-2, PSM-3

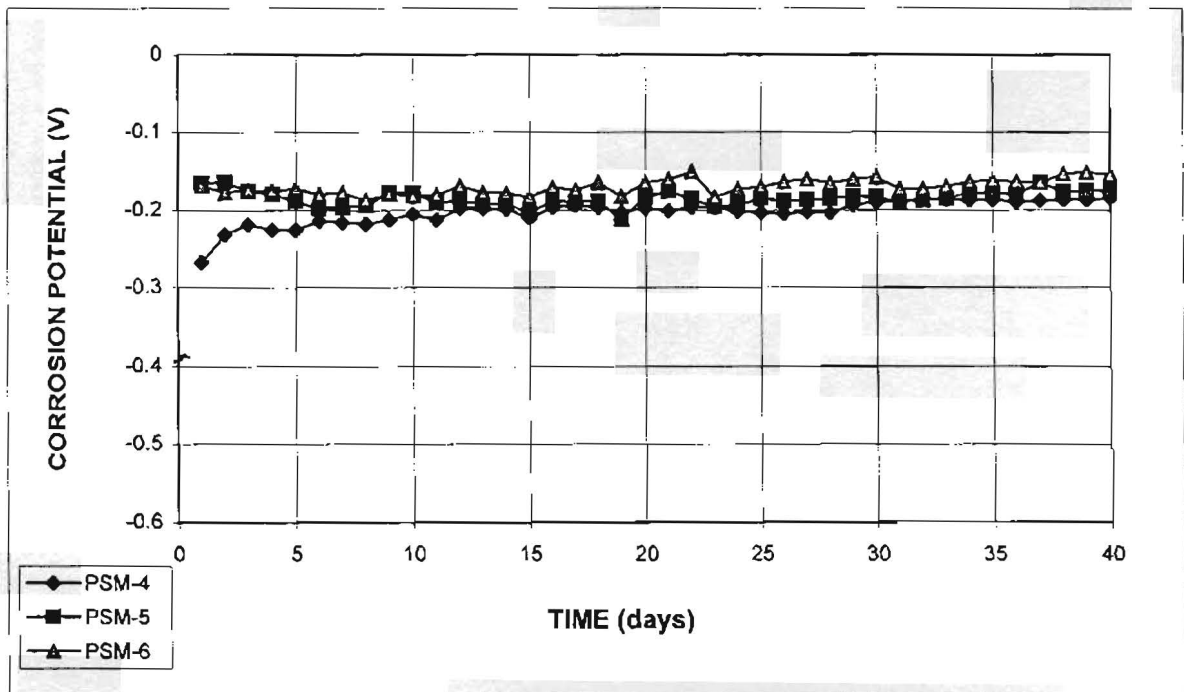


Figure 33 - Corrosion Potential Test: Stainless steel clad with mortar  
Specimens PSM-4, PSM-5, PSM-6

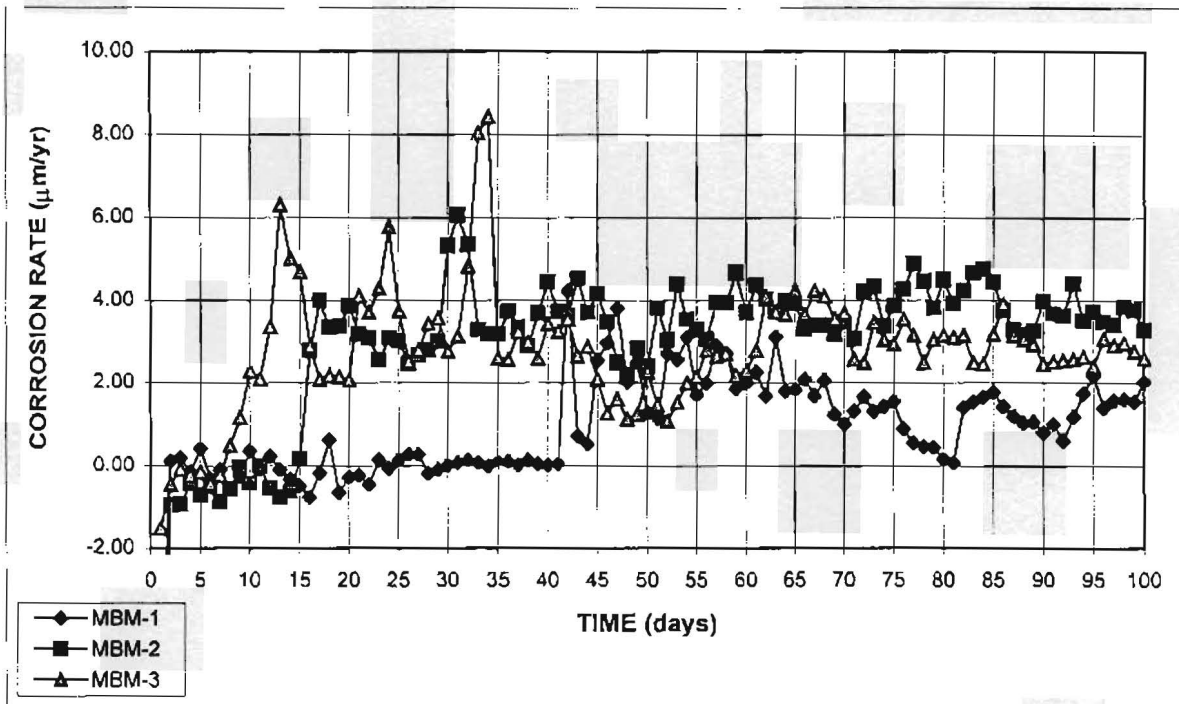


Figure 34 - Macrocell Test: Black steel with mortar. Specimens MBM-1, MBM-2 and MBM-3

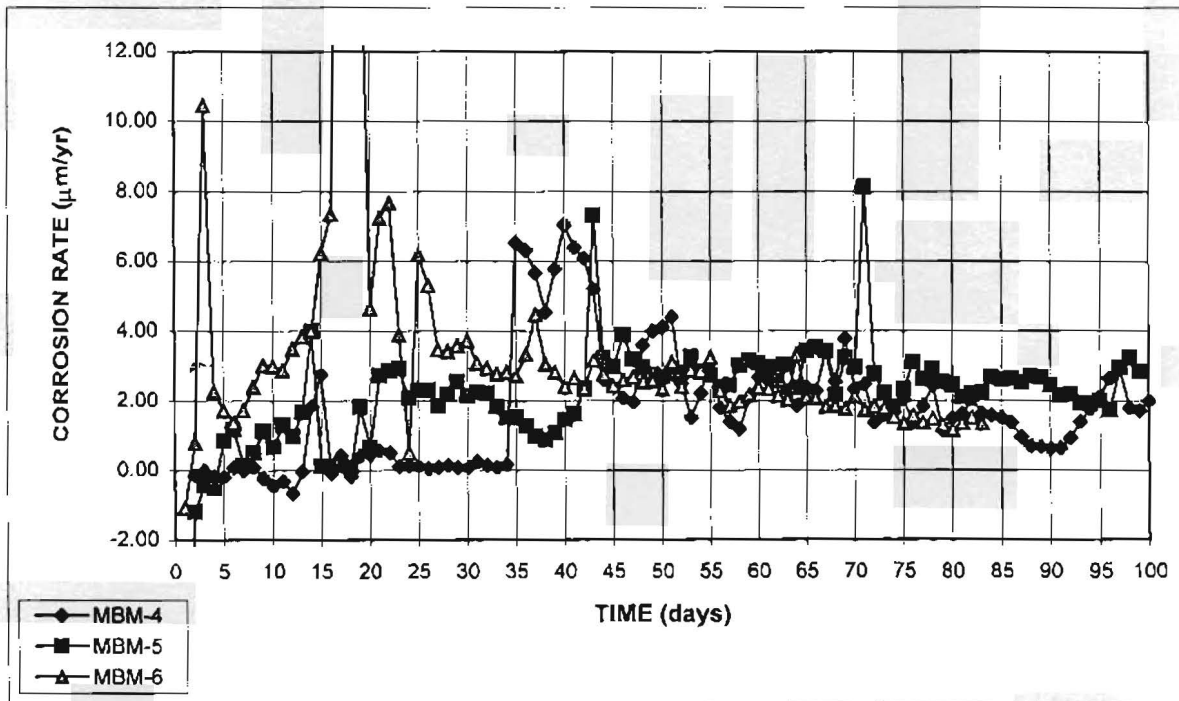


Figure 35 - Macrocell Test: Black steel with mortar. Specimens MBM-4, MBM-5 and MBM-6

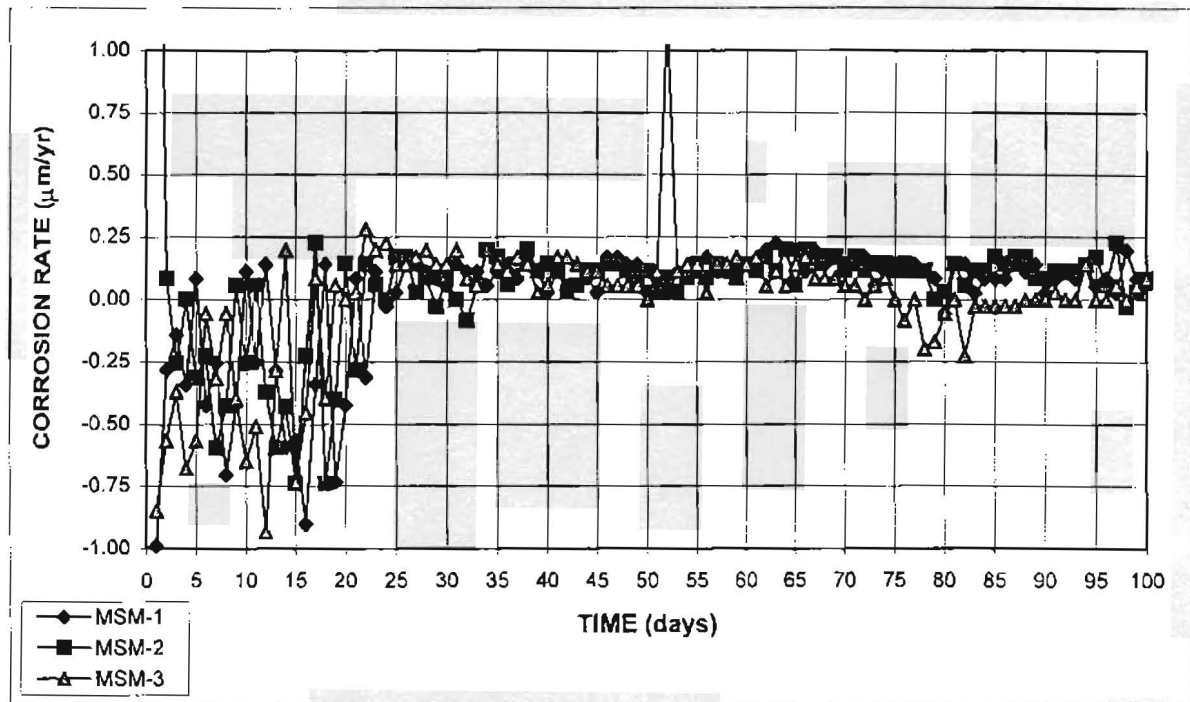


Figure 36 - Macrocell Test: Stainless steel clad with mortar.  
Specimens MSM-1, MSM-2 and MSM-3

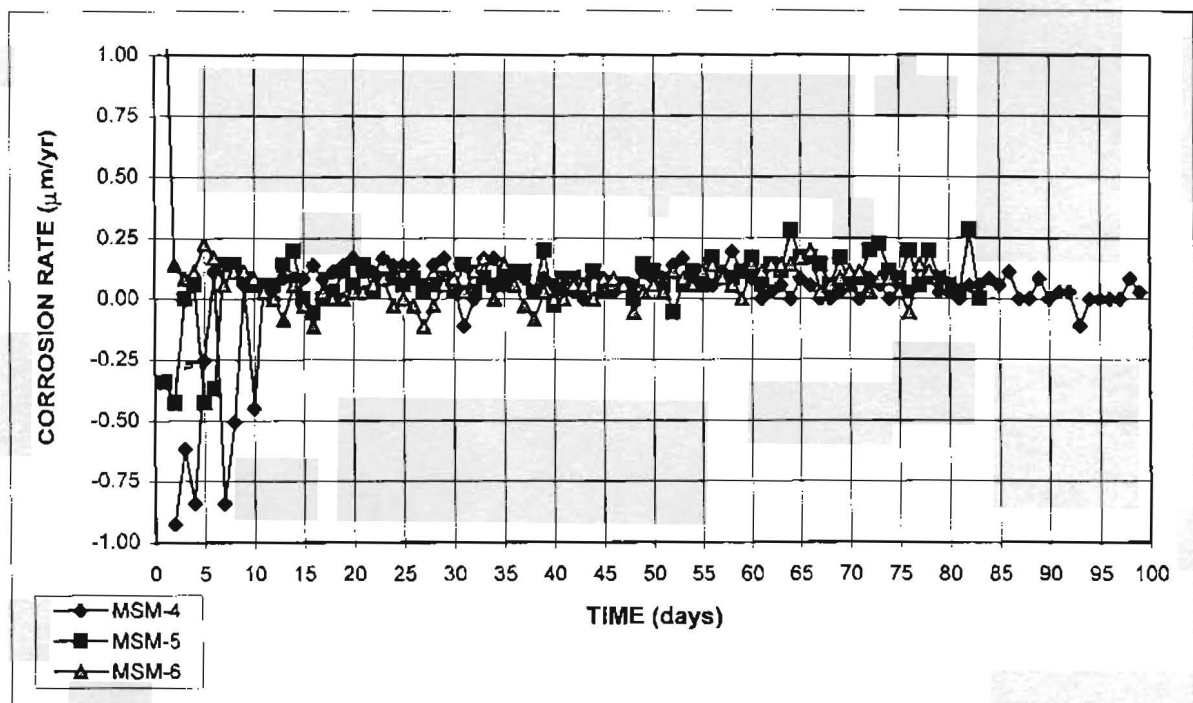
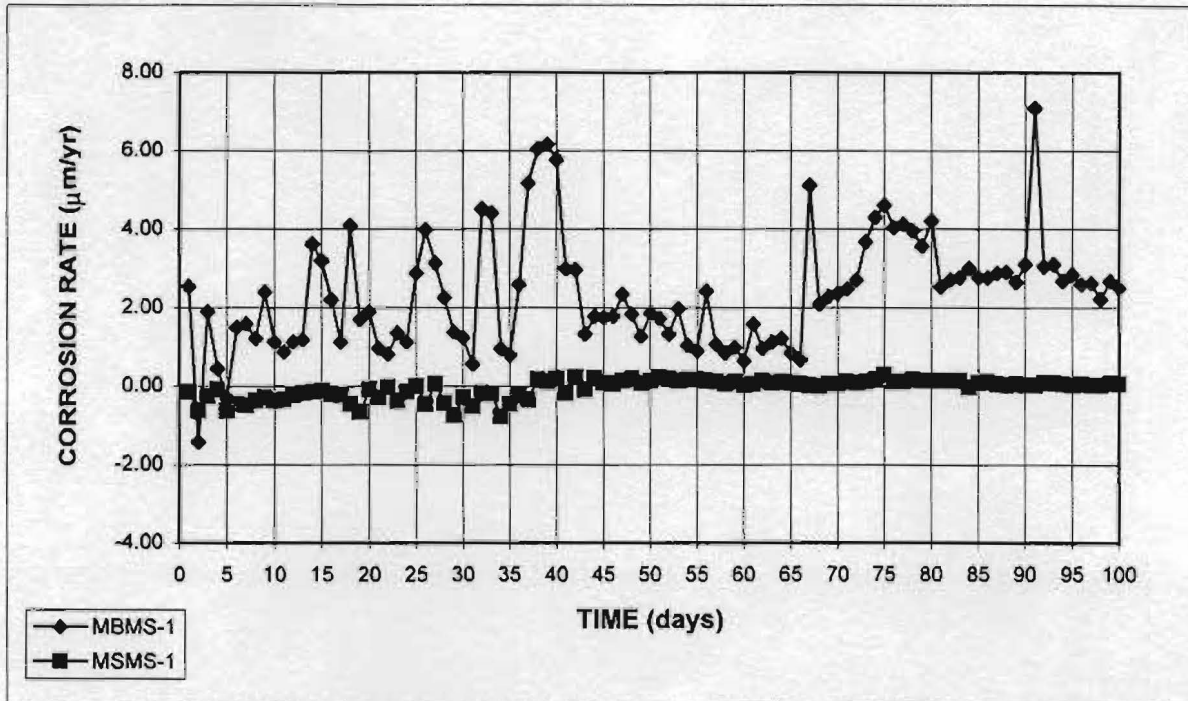
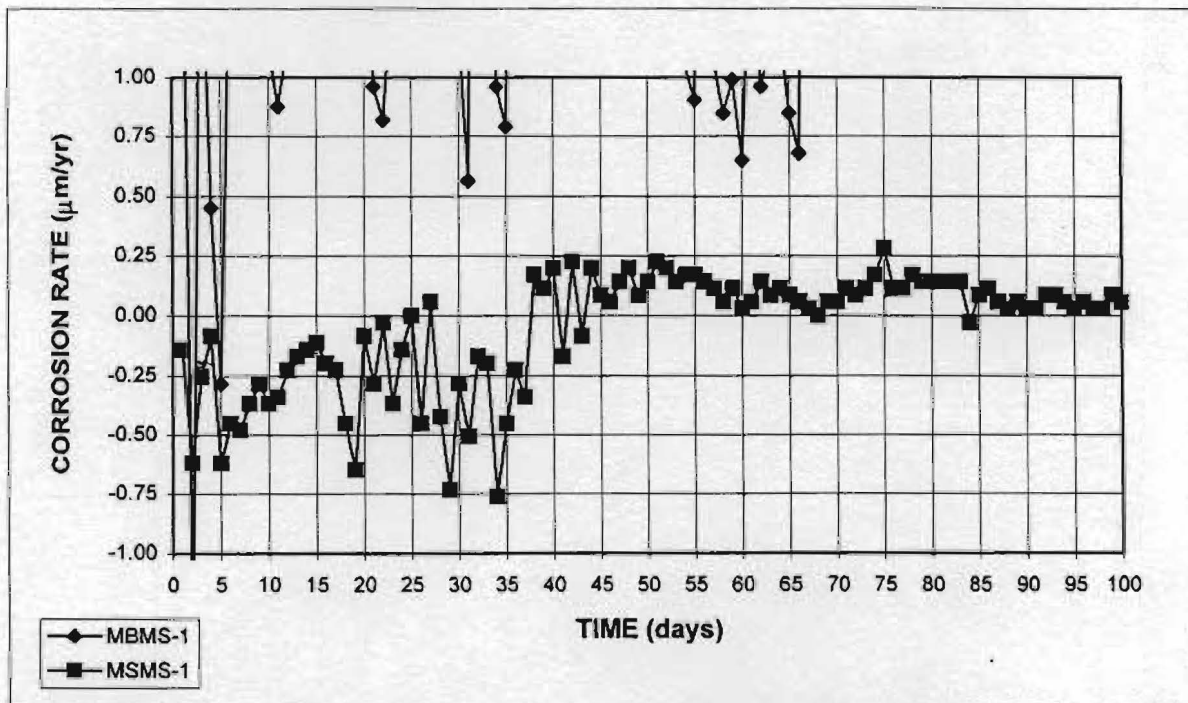


Figure 37 - Macrocell Test: Stainless steel clad with mortar.  
Specimens MSM-4, MSM-5 and MSM-6



**Figure 38a** - Macrocell Test: Black bar with mortar (Specimen MBMS-1) and stainless steel clad with mortar (Specimen MSMS-1). Small cover [Diameter of mortar cylinder = 30 mm. (1.18 in)]



**Figure 38b** - Macrocell Test: Black bar with mortar (Specimen MBMS-1) and stainless steel clad with mortar (Specimen MSMS-1). Small cover [Diameter of mortar cylinder = 30 mm. (1.18 in)]

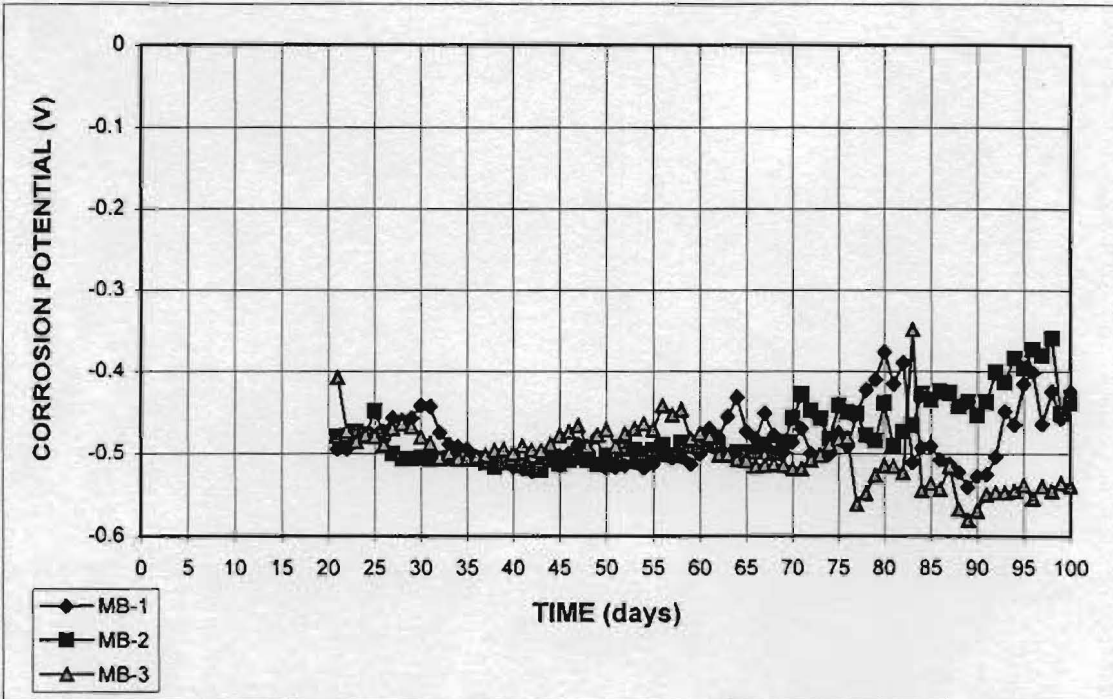


Figure A.1 - Anode Potential: Black steel without mortar. Specimens MB-1, MB-2 and MB-3

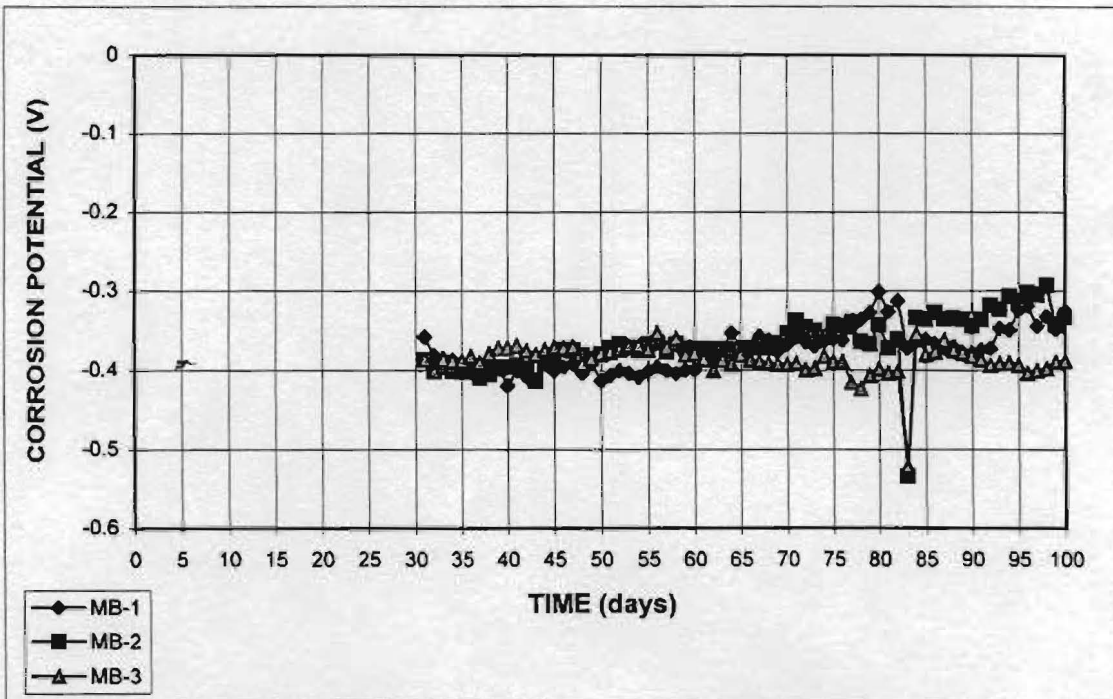


Figure A.2 - Cathode Potential: Black steel without mortar. Specimens MB-1, MB-2 and MB-3



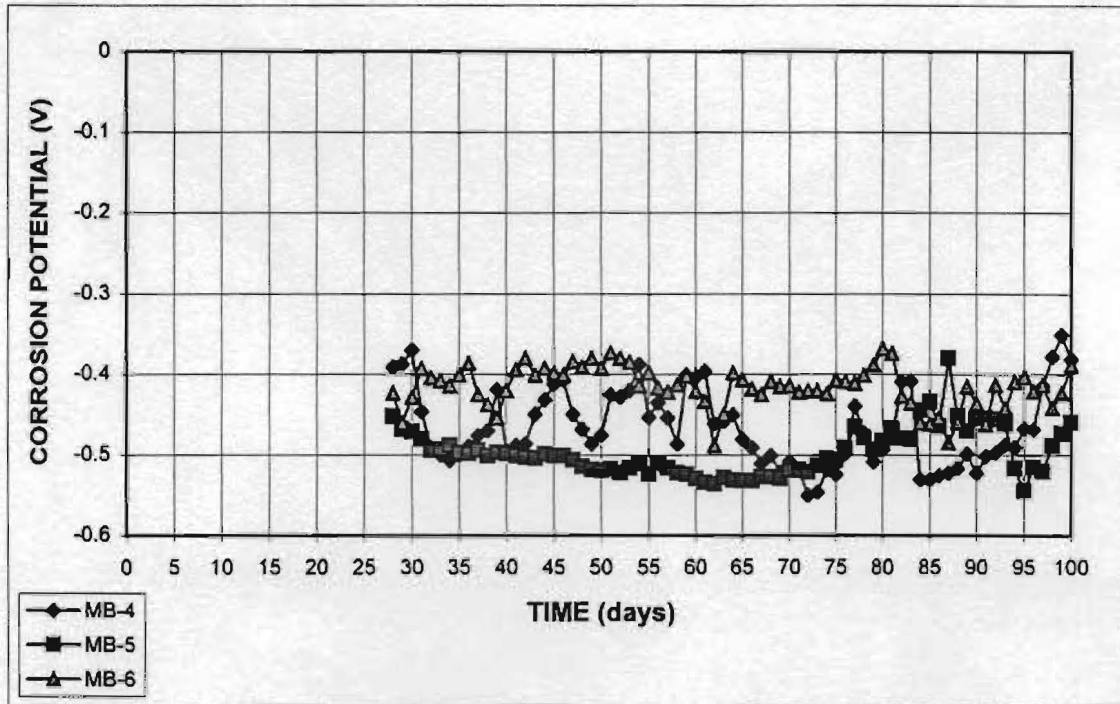


Figure A.3 - Anode Potential: Black steel without mortar. Specimens MB-4, MB-5 and MB-6

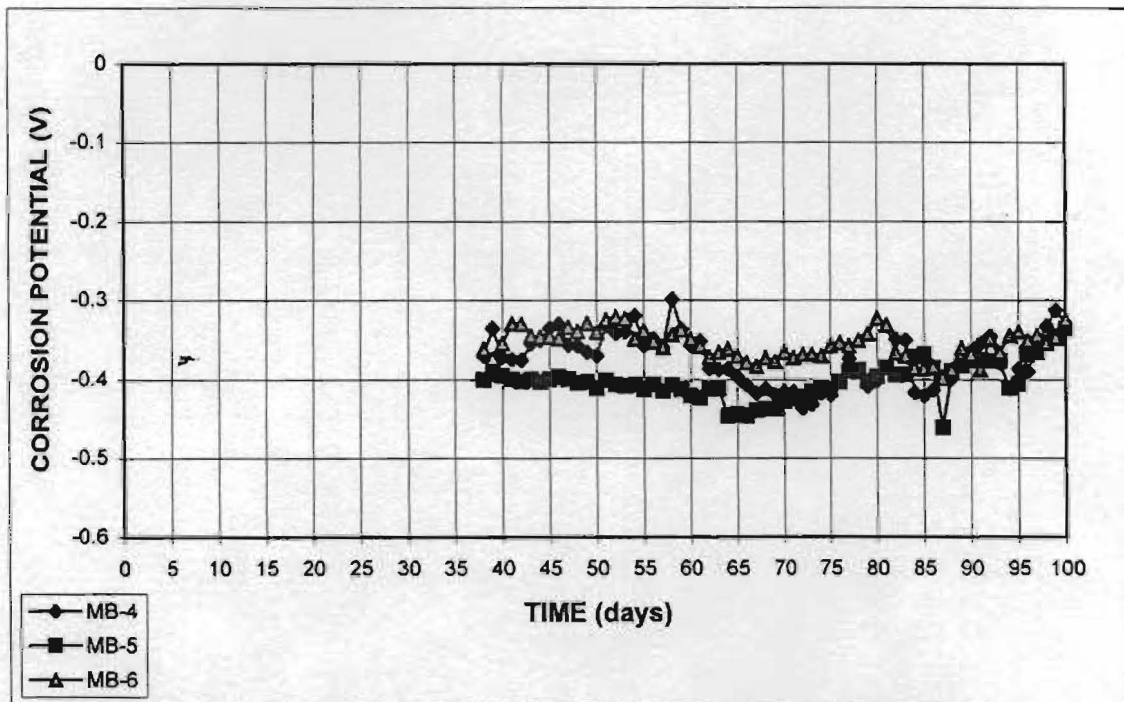


Figure A.4 - Cathode Potential: Black steel without mortar. Specimens MB-4, MB-5 and MB-6

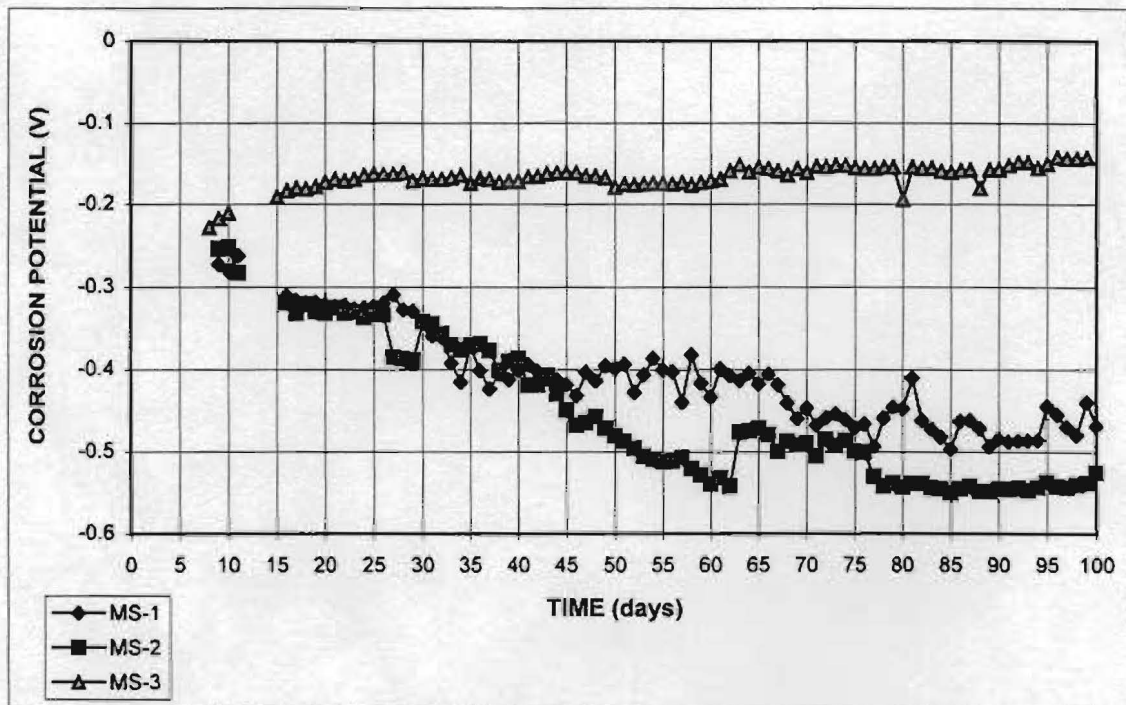


Figure A.5 - Anode Potential: Stainless steel clad without mortar.  
Specimens MS-1, MS-2 and MS-3

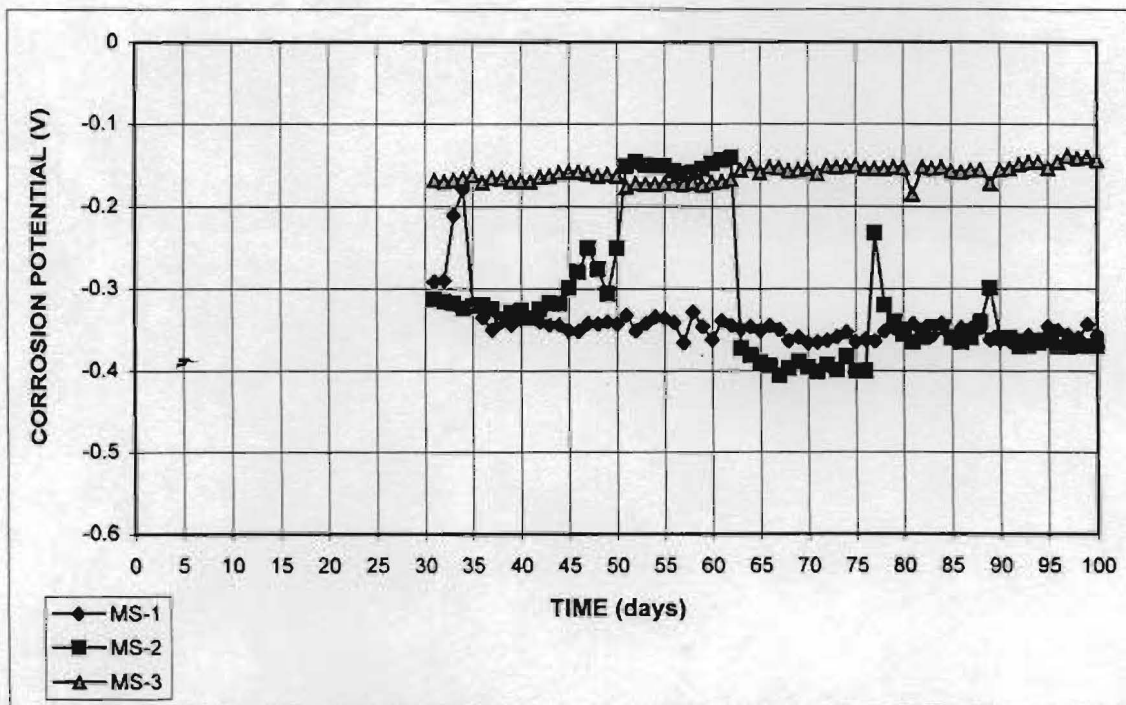


Figure A.6 - Cathode Potential: Stainless steel clad without mortar.  
Specimens MS-1, MS-2 and MS-3



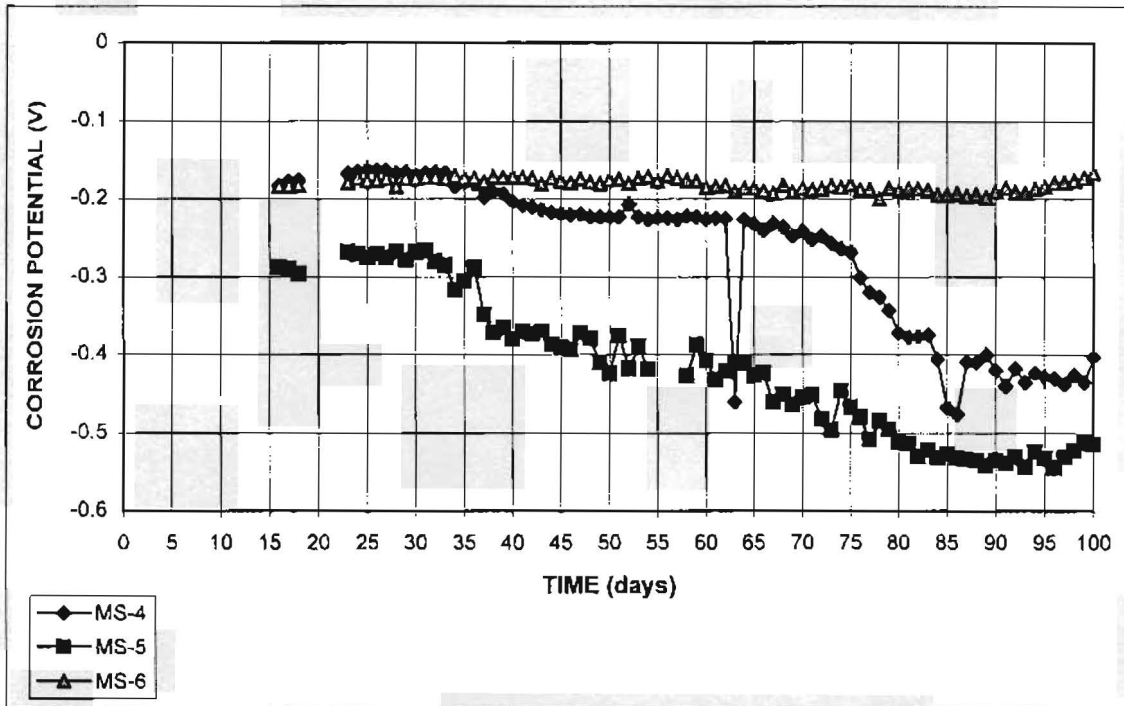


Figure A.7 - Anode Potential: Stainless steel clad without mortar.  
Specimens MS-4, MS-5 and MS-6

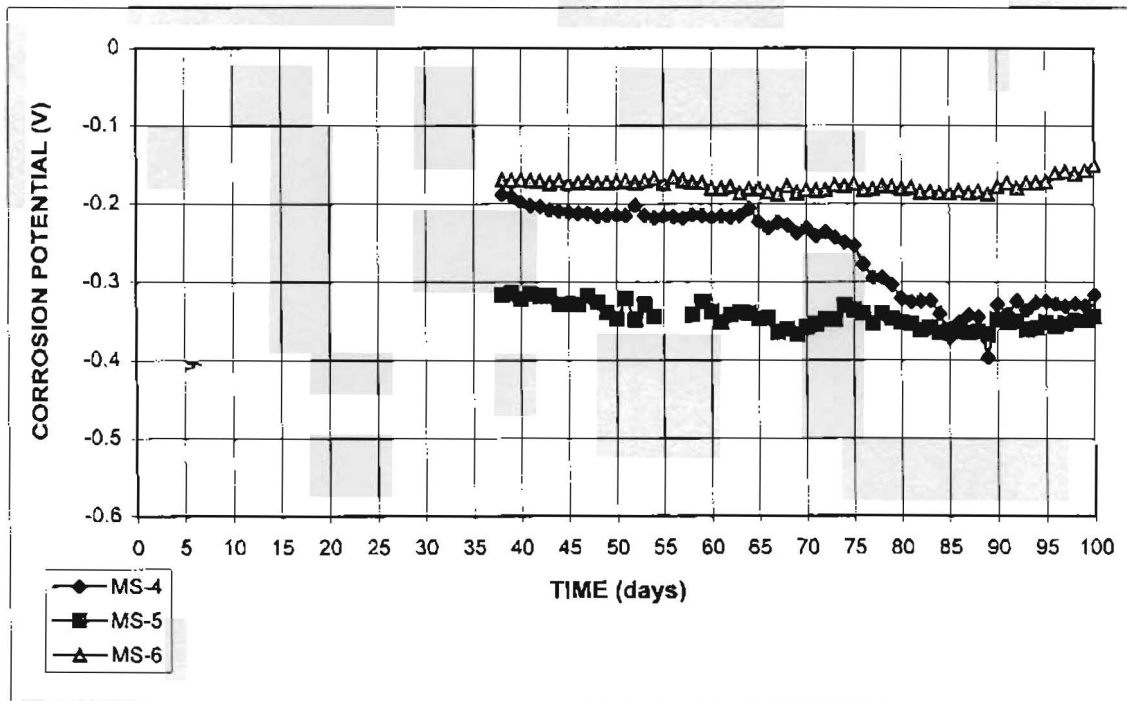


Figure A.8 - Cathode Potential: Stainless steel clad without mortar.  
Specimens MS-4, MS-5 and MS-6

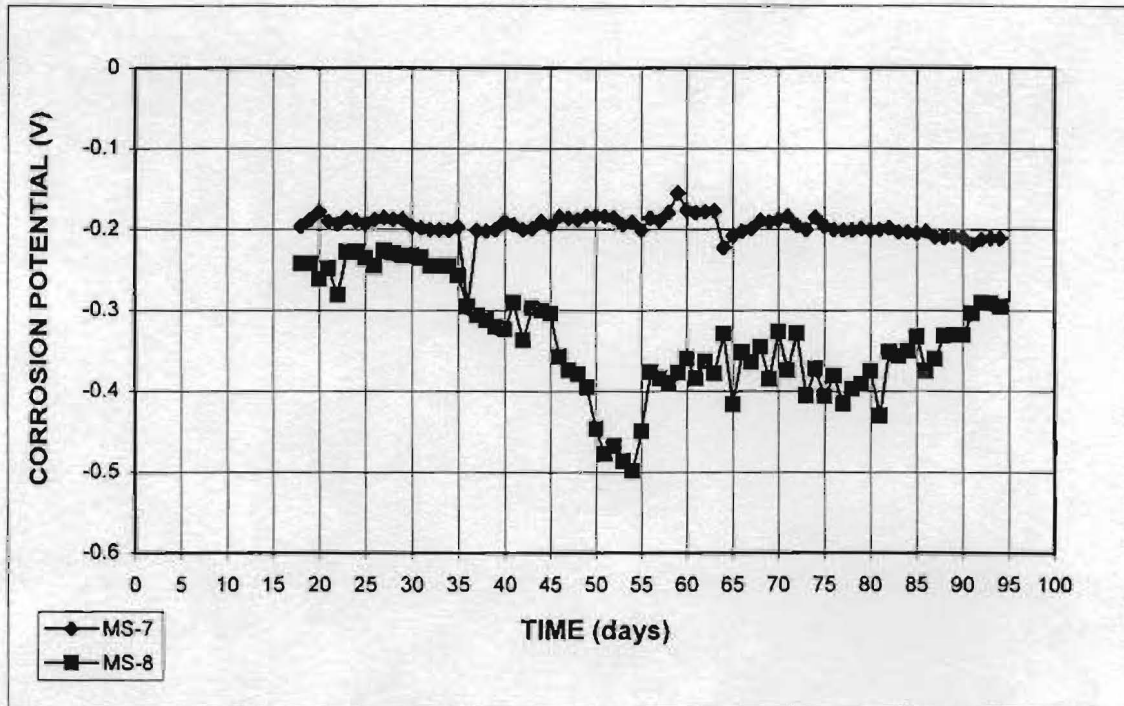


Figure A.9 - Anode Potential: Stainless steel clad without mortar.  
Specimens MS-7 and MS-8

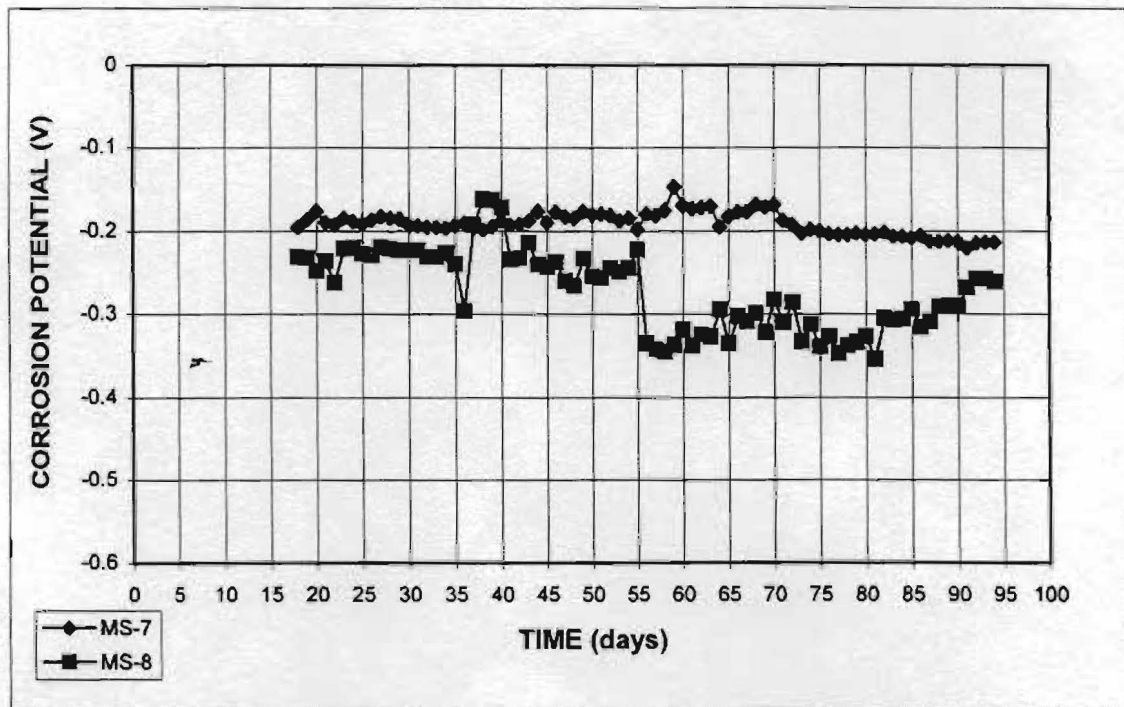


Figure A.10 - Cathode Potential: Stainless steel clad without mortar.  
Specimens MS-7 and MS-8

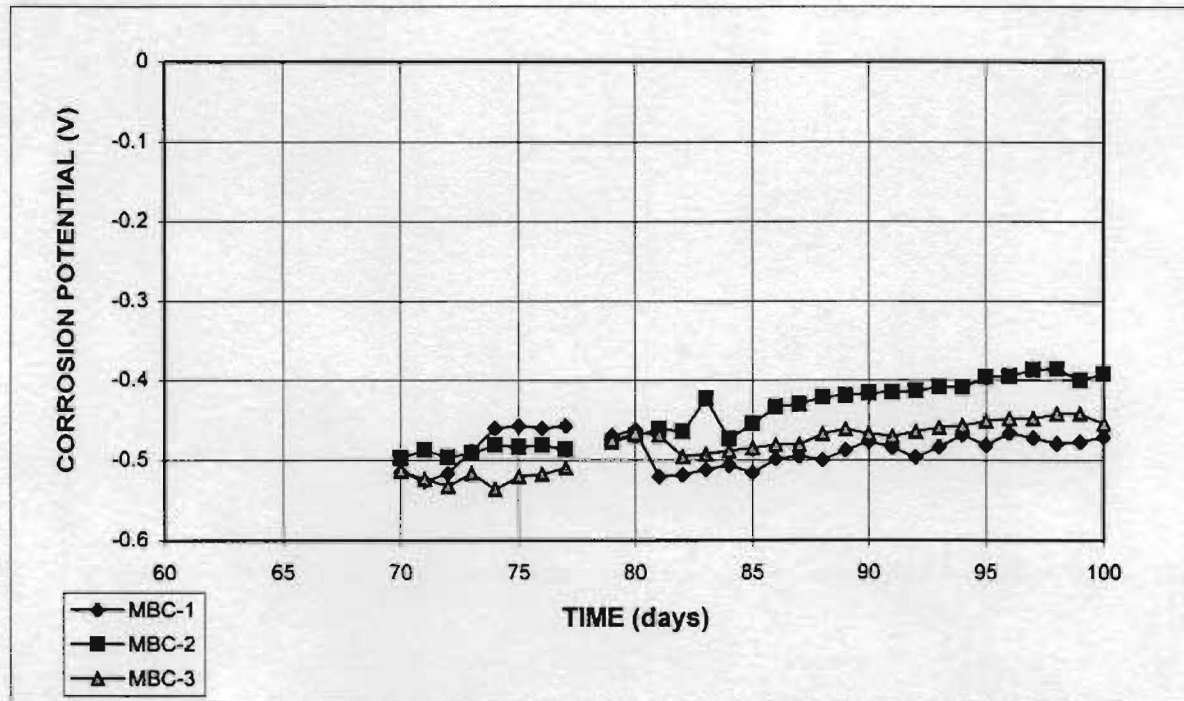


Figure A.11 - Anode Potential: Black steel without mortar, with caps.  
Specimens MBC-1, MBC-2 and MBC-3

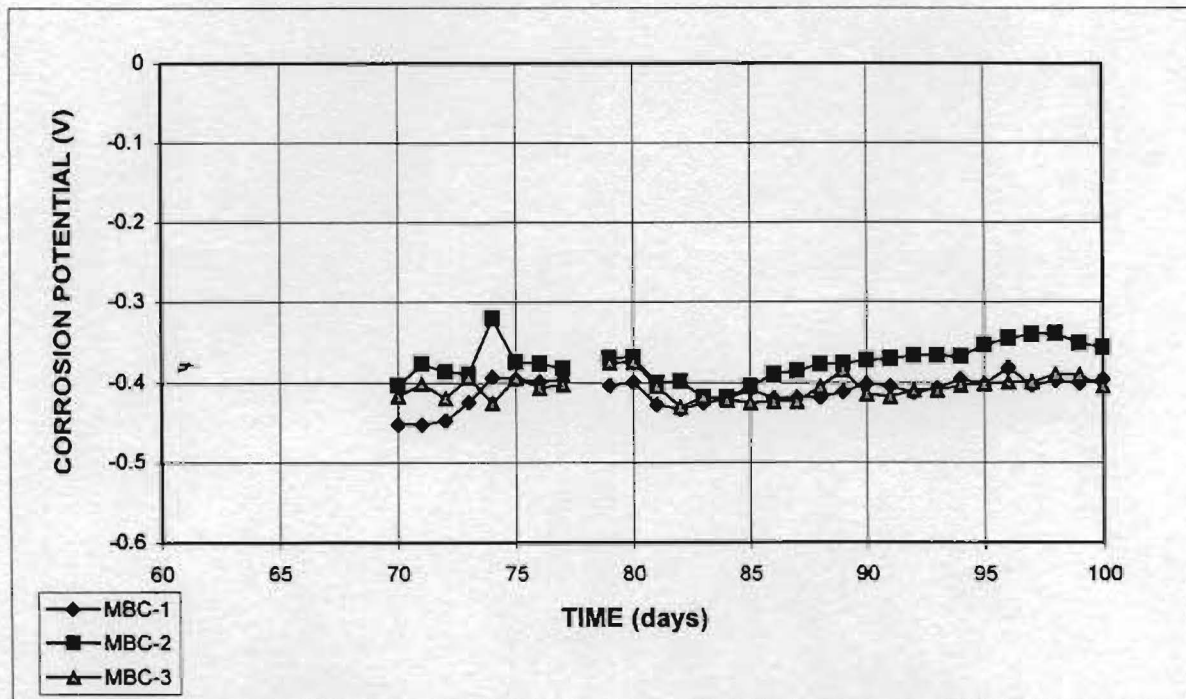
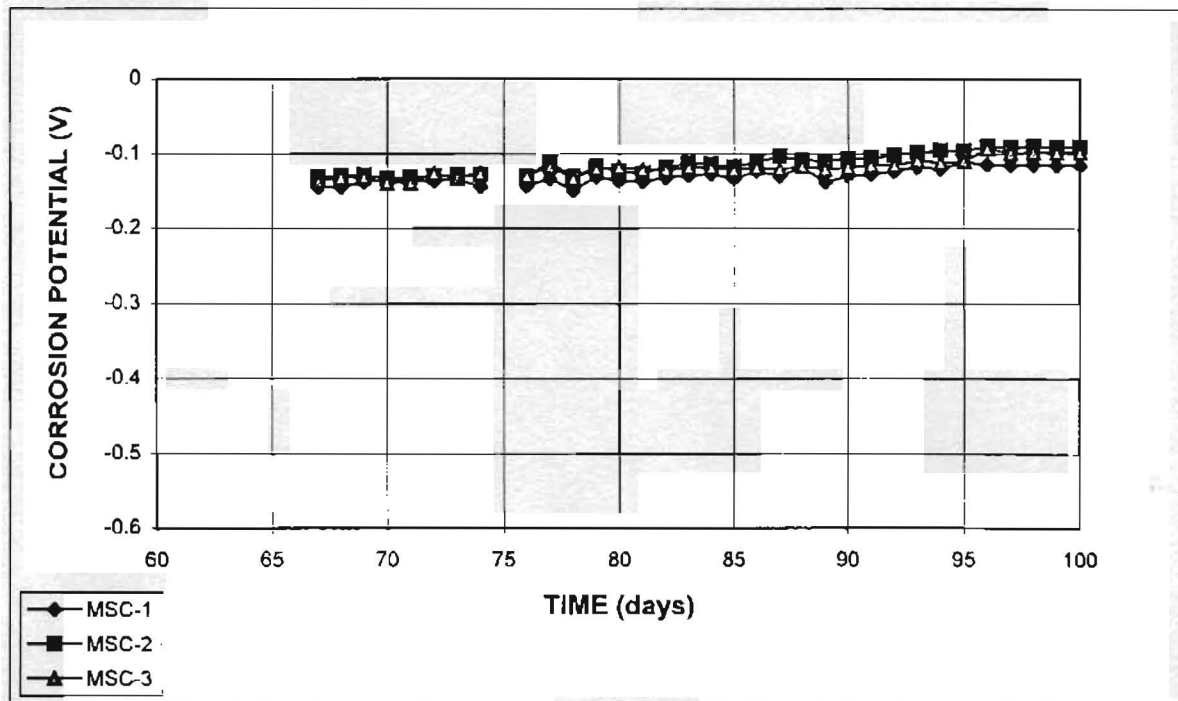
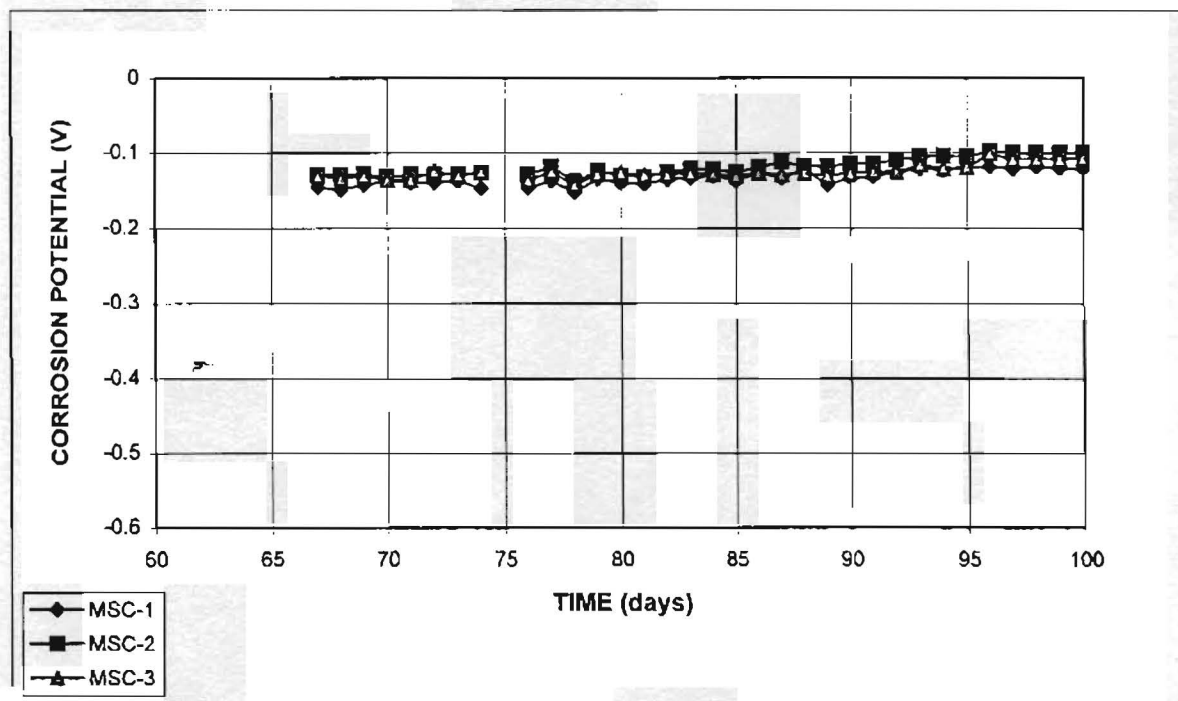


Figure A.12 - Cathode Potential: Black steel without mortar, with caps.  
Specimens MBC-1, MBC-2 and MBC-3



**Figure A.13** - Anode Potential: Stainless steel clad without mortar, with caps.  
Specimens MSC-1, MSC-2 and MSC-3



**Figure A.14** - Cathode Potential: Stainless steel clad without mortar, with caps.  
Specimens MSC-1, MSC-2 and MSC-3

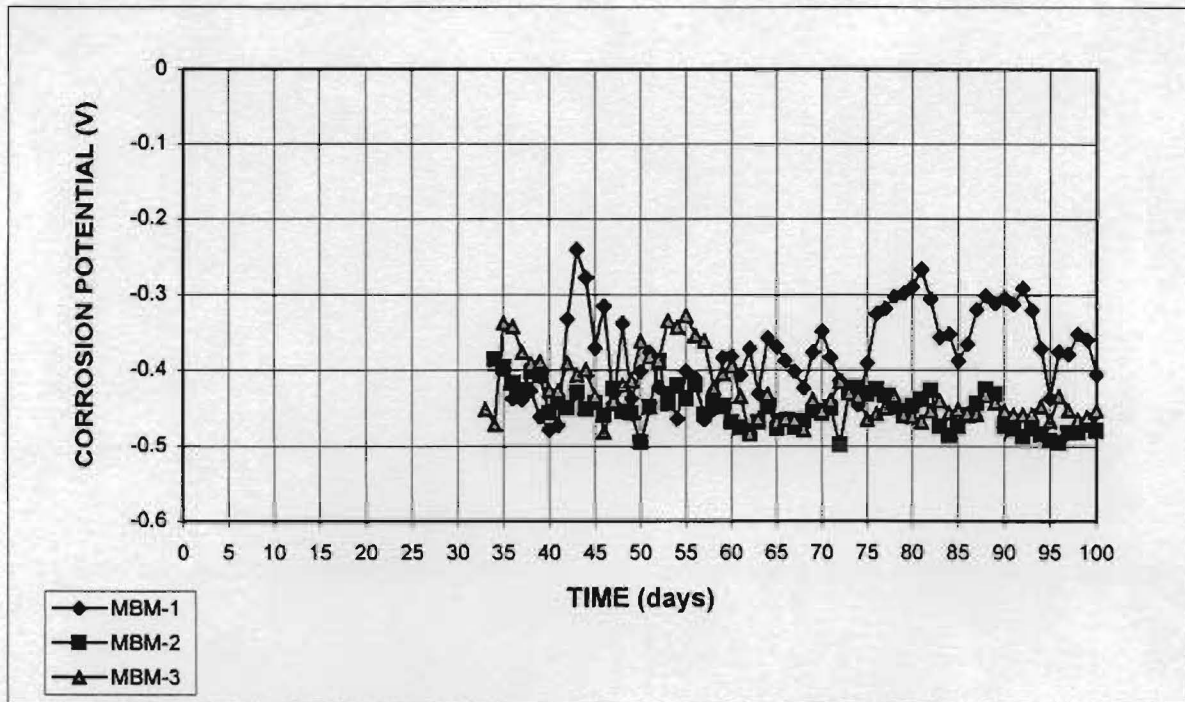


Figure A.15 - Anode Potential: Black steel with mortar. Specimens MBM-1, MBM-2 and MBM-3

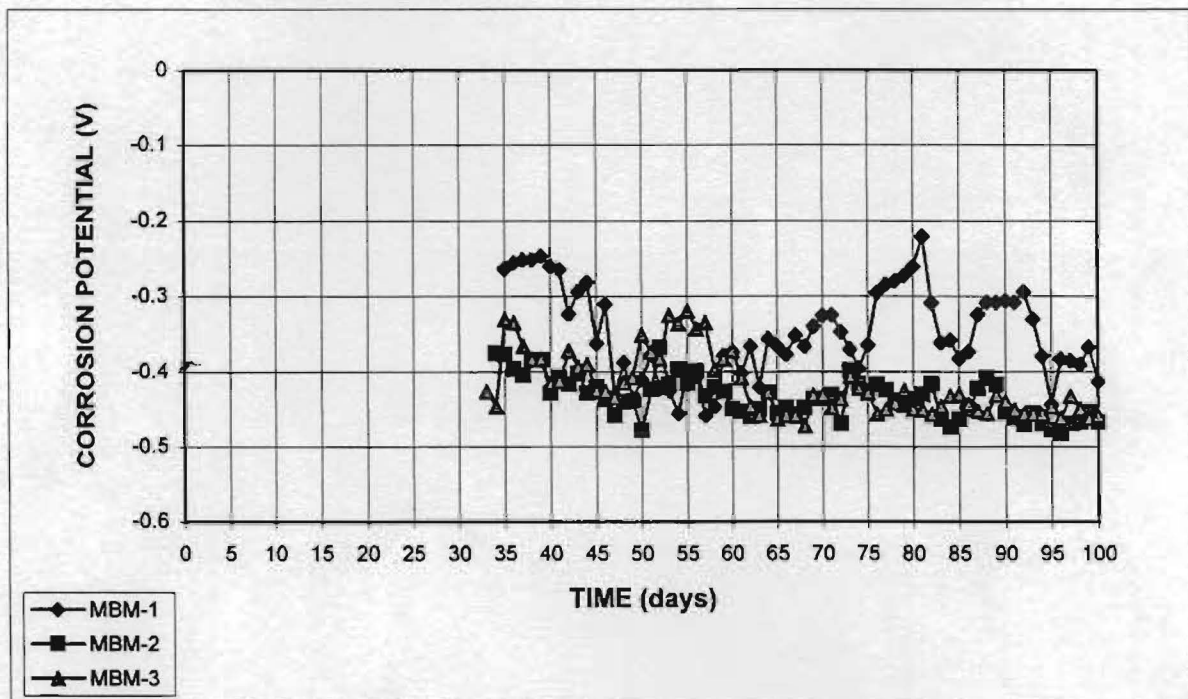


Figure A.16 - Cathode Potential: Black steel with mortar. Specimens MBM-1, MBM-2 and MBM-3



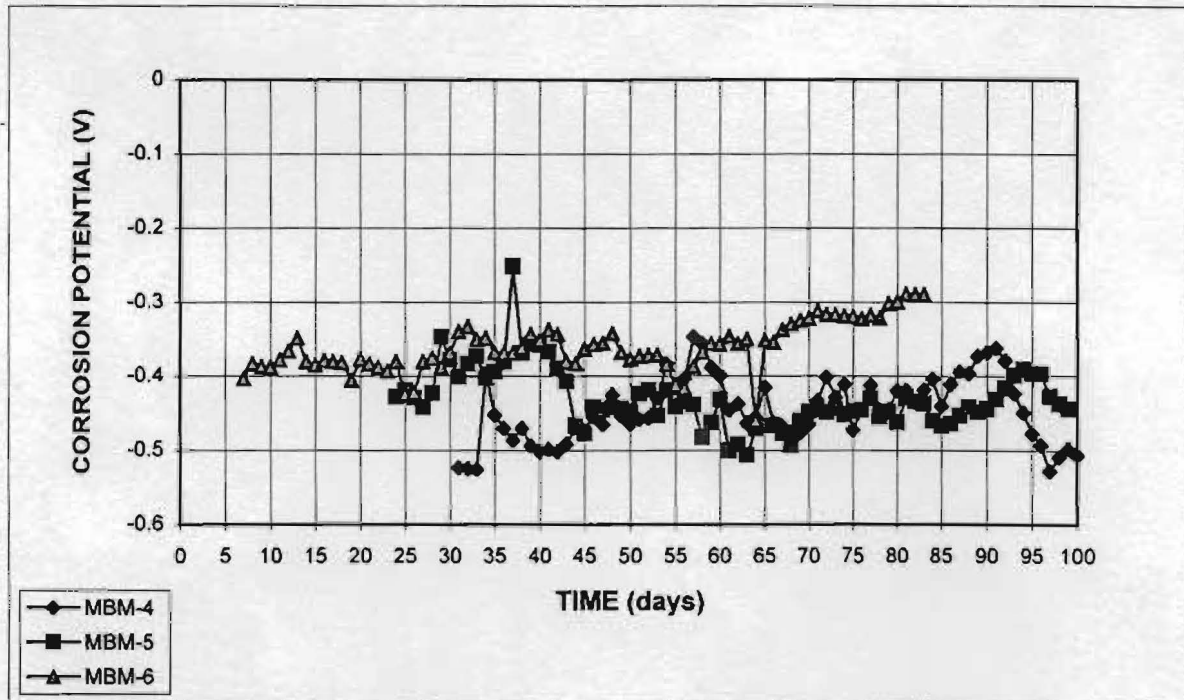


Figure A.17 - Anode Potential: Black steel with mortar. Specimens MBM-4, MBM-5 and MBM-6

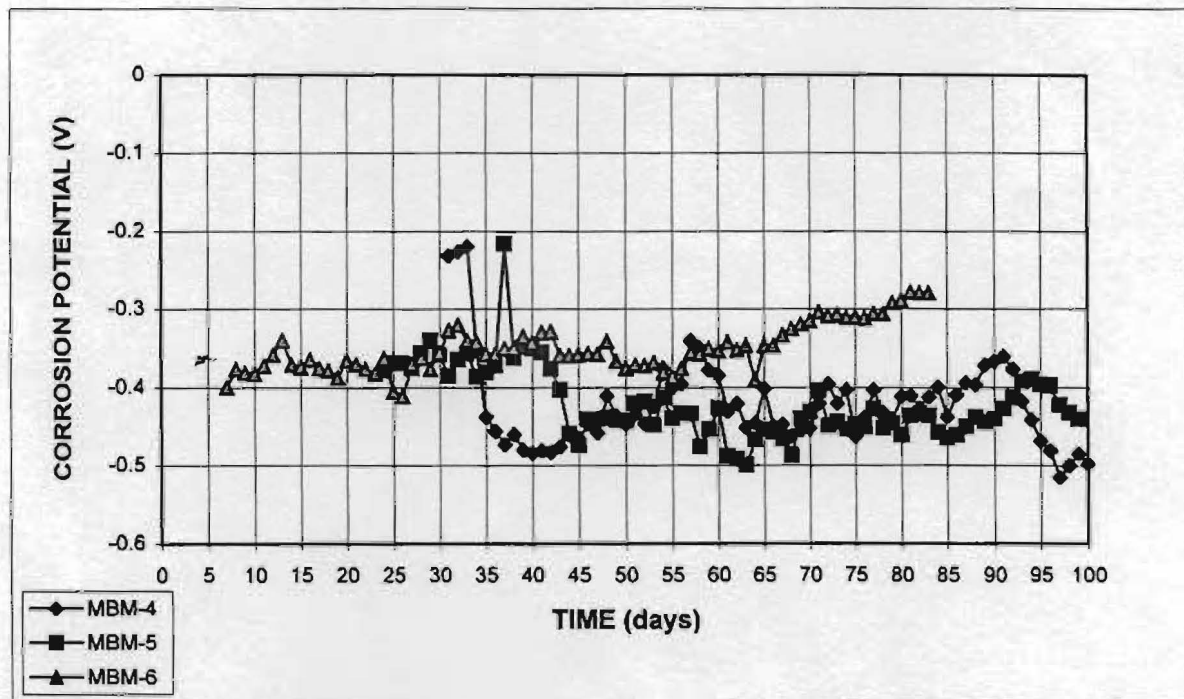


Figure A.18 - Cathode Potential: Black steel with mortar. Specimens MBM-4, MBM-5 and MBM-6

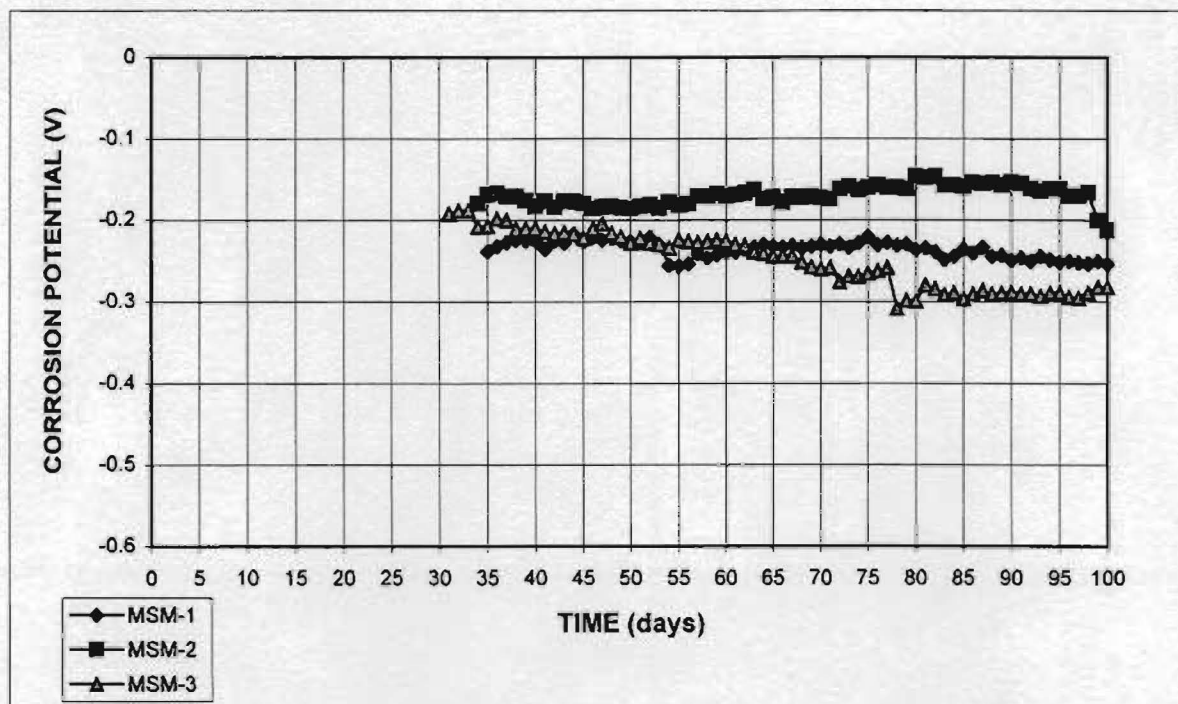


Figure A.19 - Anode Potential: Stainless steel clad with mortar.  
Specimens MSM-1, MSM-2 and MSM-3

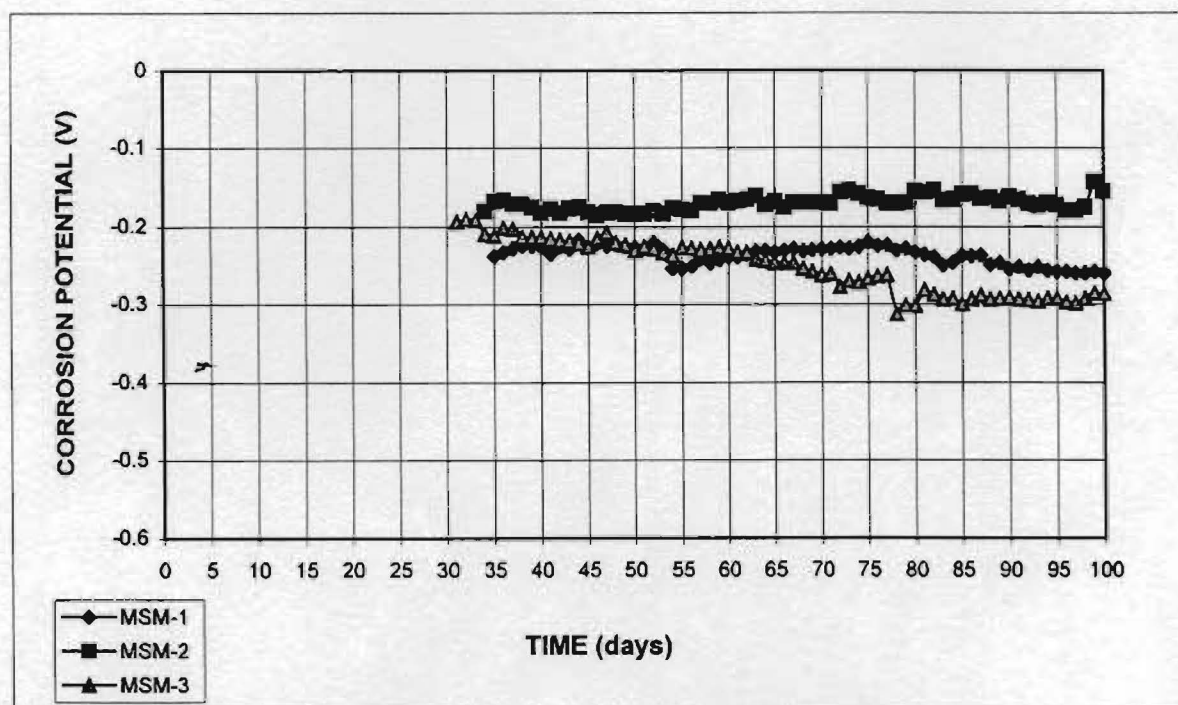


Figure A.20 - Cathode Potential: Stainless steel clad with mortar.  
Specimens MSM-1, MSM-2 and MSM-3



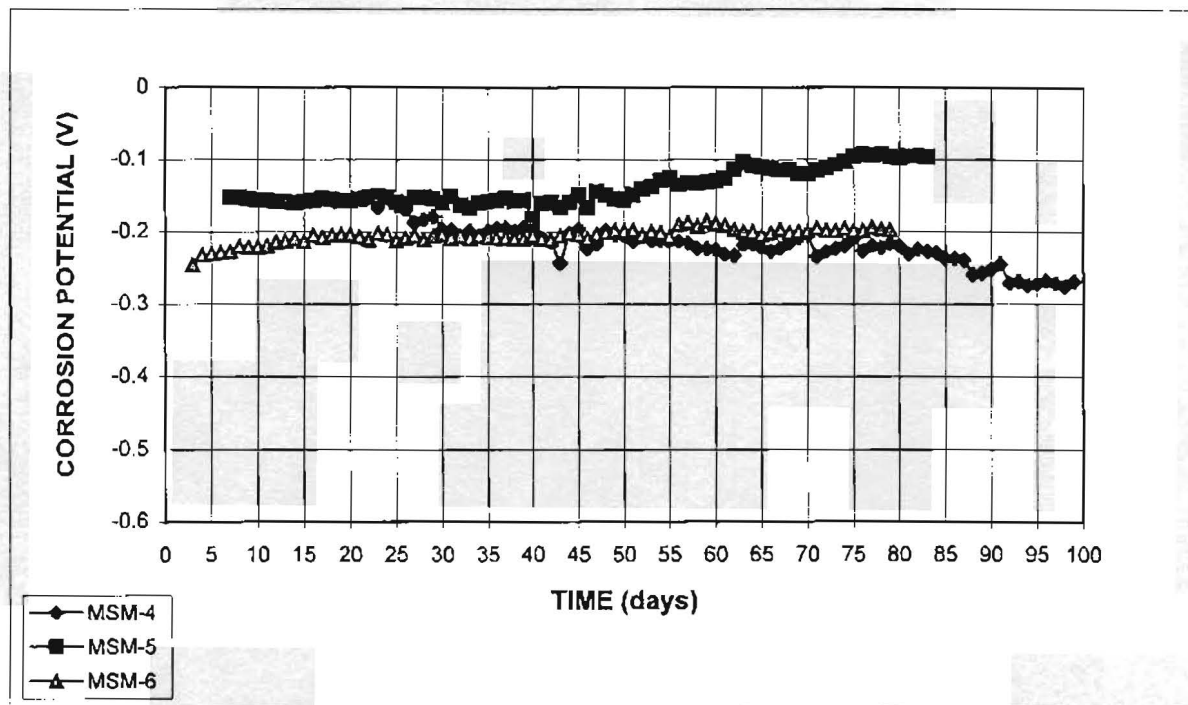


Figure A.21 - Anode Potential: Stainless steel clad with mortar.  
Specimens MSM-4, MSM-5 and MSM-6

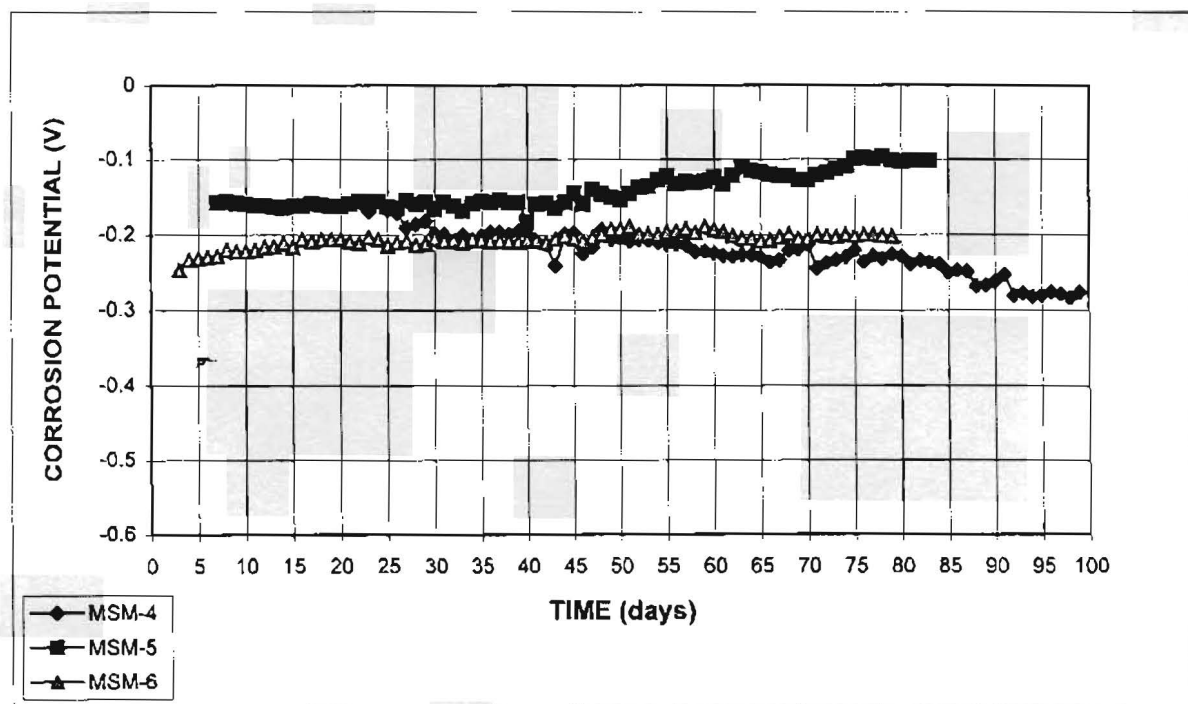


Figure A.22 - Cathode Potential: Stainless steel clad with mortar.  
Specimens MSM-4, MSM-5 and MSM-6

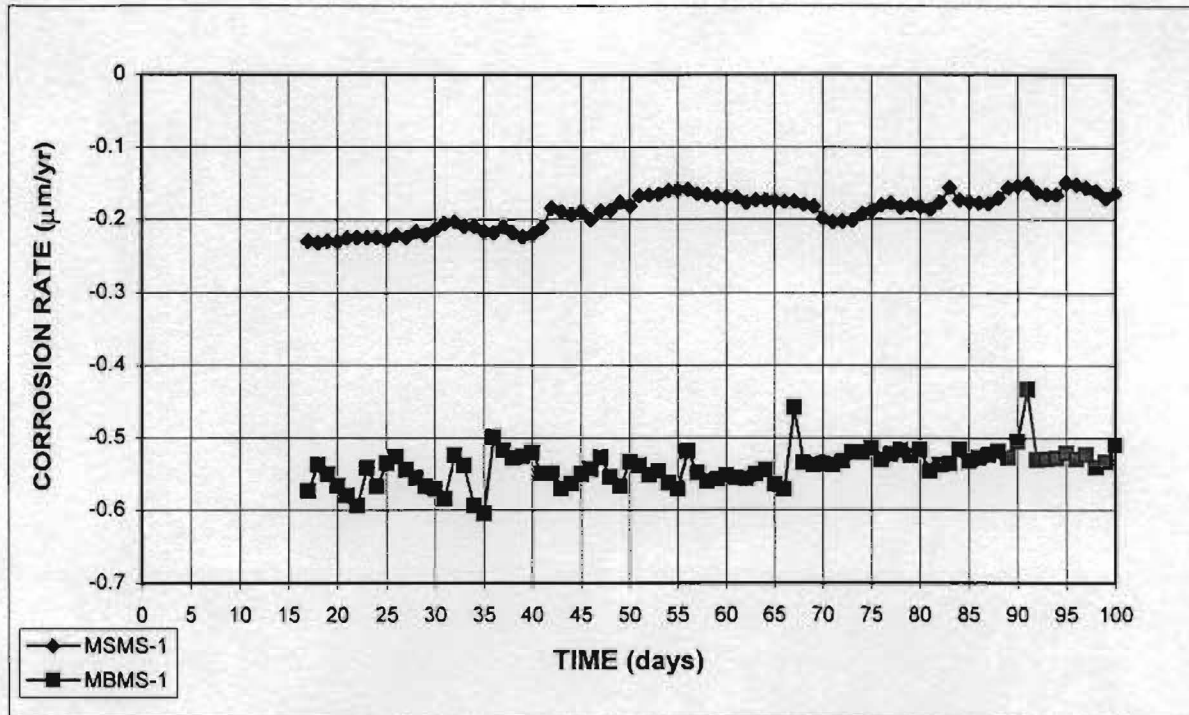


Figure A.23 - Anode Potential. Specimens with small cover (MSMS-1 and MBMS-1)

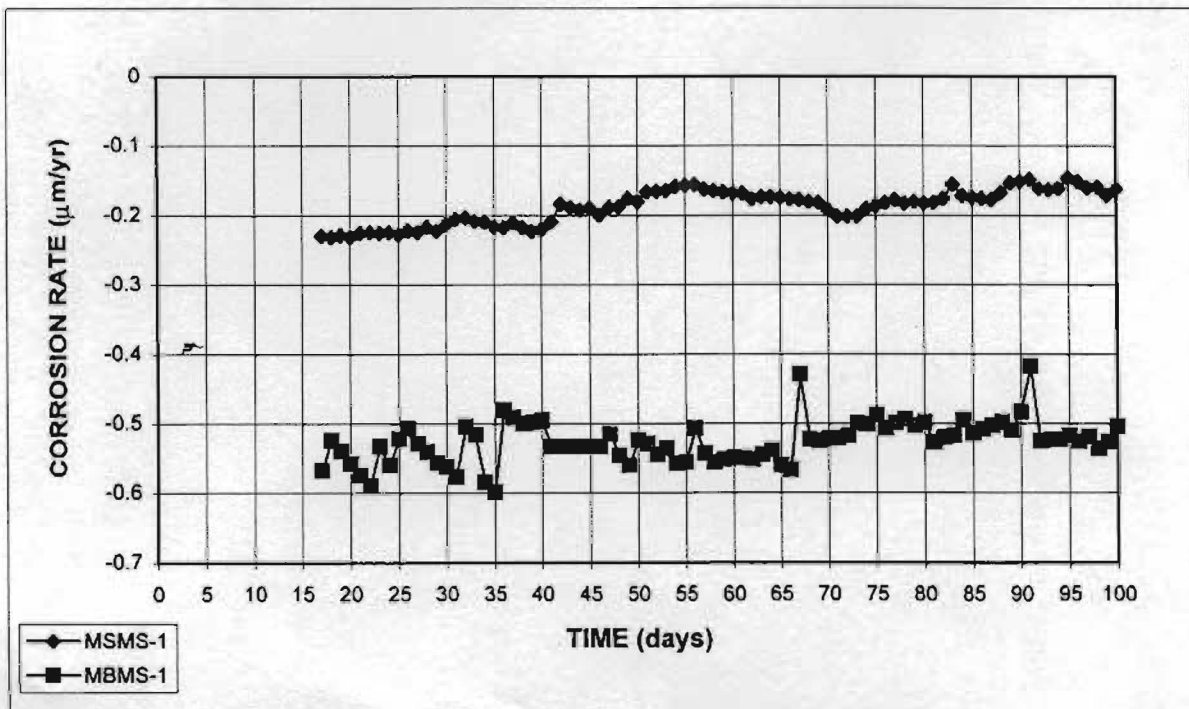


Figure A.24 - Cathode Potential. Specimens with small cover (MSMS-1 and MBMS-1)